Department of Communications and Networking

Statistical Analysis of Cascaded Multipath Fading Channels

Zhong Zheng

Aalto University

DOCTORAL DISSERTATIONS

Aalto University publication series
DOCTORAL DISSERTATIONS 209/2015

Statistical Analysis of Cascaded Multipath Fading Channels

Zhong Zheng

A doctoral dissertation completed for the degree of Doctor of Science (Technology) to be defended, with the permission of the Aalto University School of Electrical Engineering, at a public examination held at the lecture hall S3 of the school on 17 December 2015 at 12 noon.

Aalto University
School of Electrical Engineering
Department of Communications and Networking

Supervising professor
Prof. Jyri Hämäläinen

Thesis advisor
Prof. Jyri Hämäläinen

Preliminary examiners
Prof. Mérouane Debbah, CentraleSupelec, France
Prof. Sergey Loyka, University of Ottawa, Canada

Opponent
Dr. Antonia Maria Tulino, Bell Labs, USA

Aalto University publication series
DOCTORAL DISSERTATIONS 209/2015

© Zhong Zheng

ISBN 978-952-60-6562-5 (printed)
ISBN 978-952-60-6563-2 (pdf)
ISSN-L 1799-4934
ISSN 1799-4934 (printed)
ISSN 1799-4942 (pdf)
http://urn.fi/URN:ISBN:978-952-60-6563-2

Unigrafia Oy
Helsinki 2015

Finland

441 697
Printed matter

Aalto University

Abstract

Aalto University, P.O. Box 11000, FI-00076 Aalto www.aalto.fi

Author
Zhong Zheng

Name of the doctoral dissertation
Statistical Analysis of Cascaded Multipath Fading Channels

Publisher School of Electrical Engineering

Unit Department of Communications and Networking

Series Aalto University publication series DOCTORAL DISSERTATIONS 209/2015

Field of research Communications Engineering

Manuscript submitted 8 May 2015 **Date of the defence** 17 December 2015

Permission to publish granted (date) 13 November 2015 **Language** English

☐ **Monograph** ☒ **Article dissertation (summary + original articles)**

Abstract

In cellular communication systems, one of the prominent impairments due to the wireless channel is the multipath fading. In this thesis, we study the multipath effects, particularly in the so-called cascaded fading channels. These channel models are useful when characterizing the indoor signal propagation, time-reversal transmission, and the rank deficiency due to insufficient scattering in multiantenna communications.

Thesis focuses on the statistical performance metrics of wireless systems. More precisely, in single-antenna transmission, we analyze the received signal distribution via moment-based approximation in presence of correlated cascaded channels. Using these results, the impact of channel correlation and number of scatterers are investigated for the cascaded Nakagami-m channels. Furthermore, the signal distribution of the cascaded Rician channel is used to construct a test statistics for a blind time-reversal detector. In the presence of a point target embedded in the multipath scattering, we show by Monte Carlo simulation that the proposed detector outperforms the existing detectors.

In multi-antenna communications framework we consider information theoretic limits for the cascaded Rayleigh MIMO channels. In the ergodic channel, we obtain a lower bound for the ergodic mutual information and deduce a rate scaling law using a recent result from the random matrix theory. For the non-ergodic channel, we study the outage probability by establishing the central limit theorem for the linear spectral statistics of the channel matrices. This result also motivates us to construct a simple approximation for the fundamental tradeoff between diversity gain and multiplexing gain of the MIMO channel at realistic SNR levels.

Keywords cascaded fading channel, free probability theory, MIMO, random matrix theory, wireless communications

ISBN (printed) 978-952-60-6562-5 **ISBN (pdf)** 978-952-60-6563-2

ISSN-L 1799-4934 **ISSN (printed)** 1799-4934 **ISSN (pdf)** 1799-4942

Location of publisher Helsinki **Location of printing** Helsinki **Year** 2015

Pages 116 **urn** http://urn.fi/URN:ISBN:978-952-60-6563-2

To Chunfang and Lumi

Preface

The work for this doctoral thesis has been carried out in the Department of Communications and Networking at Aalto University, Finland. The work has been funded by the Graduate School in Electronics, Telecommunications and Automation (GETA), Nokia Foundation, and the Academy of Finland.

First and foremost, I would like to express my utmost gratitude to Prof. Jyri Hämäläinen for his continuous encouragement and generous support. Prof. Hämäläinen has been a truly excellent mentor and he provided me balanced guidance and freedom to pursue the research questions. It is my great pleasure and honer to work with him during the past years.

I would like to extend my gratitude to Prof. Ralf Müller from University of Erlangen-Nuremberg and Prof. Roland Speicher from Saarland University for their hospitality during my visits to their groups. Their insightful comments and guidance on free probability theory have made several publications possible. I would also like to thank Dr. Lu Wei for the numerous and fruitful discussions. His encouragement has led me into the work of random matrix theory.

I would like to thank the thesis pre-examiners Prof. Mérouane Debbah and Prof. Sergey Loyka for their efforts in reviewing the manuscript. Their invaluable comments and suggestions have greatly improved the quality of the thesis. I would also like to thank Prof. Antonia Tulino for accepting to be the defense opponent.

I would also like to thank my coauthors: Prof. Jukka Corander, Dr. Alexis Dowhuszko, Mr. Mika Husso, Dr. Timo Korhonen, Dr. Edward Mutafungwa, Prof. Giorgio Taricco, Prof. Olav Tirkkonen, and Mr. Inam Ullah. I'm sincerely appreciated all of your contributions. The COMNET secretaries and supporting team are also acknowledged for making our everyday life easier. Special thanks to Prof. Zygmunt Haas for giving me

the opportunity to pursue my research direction.

Last, but not least, I would like to thank my wife Chunfang Tang for her understanding and love during the past few years. Her support and encouragement was in the end what made this dissertation possible. My parents, Tingjun Zheng and Weiwei He, receive my deepest gratitude and love for their dedication and the many years of support during my studies that provided the foundation for this work.

Richardson, USA, November 16, 2015,

Zhong Zheng

Contents

List of Publications

This thesis consists of an overview and of the following publications which are referred to in the text by their Roman numerals.

I Zhong Zheng, Lu Wei, Jyri Hämäläinen, and Olav Tirkkonen. Approximation to distribution of product of random variables using orthogonal polynomials for lognormal density. *IEEE Communications Letters*, vol. 16, no. 12, pp. 2028-2031, Dec. 2012.

II Zhong Zheng, Lu Wei, and Jyri Hämäläinen. Novel approximations to the statistics of general cascaded Nakagami-m channels and their applications in performance analysis. In *Proceedings of IEEE International Conference on Communications*, Budapest, Hungary, pp. 5835-5839, June 2013.

III Zhong Zheng, Lu Wei, Jyri Hämäläinen, and Olav Tirkkonen. A blind time-reversal detector in the presence of channel correlation. *IEEE Signal Processing Letters*, vol. 20, no. 5, pp. 459-462, May 2013.

IV Lu Wei, Zhong Zheng, Olav Tirkkonen, and Jyri Hämäläinen. On the ergodic mutual information of multiple cluster scattering MIMO channels. *IEEE Communications Letters*, vol. 17, no. 9, pp. 1700-1703, Sept. 2013.

V Zhong Zheng, Lu Wei, Roland Speicher, Ralf Müller, Jyri Hämäläinen, and Jukka Corander. On the fluctuation of mutual information in double scattering MIMO channels. In *Proceedings of International Zurich Seminar on Communications*, Zurich, Switzerland, pp. 104-107, June 2013.

VI Zhong Zheng, Lu Wei, Roland Speicher, Ralf Müller, Jyri Hämäläinen, and Jukka Corander. Outage capacity of Rayleigh product channels: a free probability approach. *IEEE Transactions on Information*

Theory, submitted on 17th Feb. 2015.

VII Zhong Zheng, Lu Wei, Roland Speicher, Ralf Müller, Jyri Hämäläinen, and Jukka Corander. On the finite-SNR diversity-multiplexing tradeoff in large Rayleigh product channels. In *Proceedings of IEEE International Symposium on Information Theory*, Hong Kong, pp. 2593-2597, June 2015.

Author's Contribution

Publication I: "Approximation to distribution of product of random variables using orthogonal polynomials for lognormal density"

The author had the main responsibility for formulating the idea, performing simulations, and writing this article. Dr. Lu Wei pointed out the moment-based approximation method and participated in deriving the results.

Publication II: "Novel approximations to the statistics of general cascaded Nakagami-m channels and their applications in performance analysis"

The author had the main responsibility for formulating the idea, performing simulations, and writing this article.

Publication III: "A blind time-reversal detector in the presence of channel correlation"

The author had the main responsibility for deriving the results, performing simulations, and writing this article. Dr. Lu Wei participated in formulating the idea of this article.

Publication IV: "On the ergodic mutual information of multiple cluster scattering MIMO channels"

The author participated in development of idea and writing of this article. The author had the main responsibility in performing simulations and

analysis of results.

Publication V: "On the fluctuation of mutual information in double scattering MIMO channels"

The author had the main responsibility for formulating the idea, performing simulations, and writing this article. Dr. Ralf Müller introduced the concept of the second order Cauchy transform. The author carried out the proof of Lemma 1 jointly with Dr. Roland Speicher and Dr. Octavio Arizmendi.

Publication VI: "Outage capacity of Rayleigh product channels: a free probability approach"

The author had the main responsibility for formulating the idea, performing simulations, and writing this article. The author carried out the proof of Proposition 2 jointly with Dr. Roland Speicher and Dr. Octavio Arizmendi.

Publication VII: "On the finite-SNR diversity-multiplexing tradeoff in large Rayleigh product channels"

The author had the main responsibility for formulating the idea, performing simulations, and writing this article.

List of Abbreviations

CDF	Cumulative Distribution Function
CLT	Central Limit Theorem
CSI	Channel State Information
DMT	Diversity-Multiplexing Tradeoff
ESD	Empirical Spectral Distribution
i.i.d.	independent and identically distributed
LRT	Likelihood Ratio Test
LSS	Linear Spectral Statistics
MI	Mutual Information
MIMO	Multi-Input Multi-Output
Pd	detection probability
PDF	Probability Density Function
Pfa	false alarm probability
PSD	Power Spectral Density
ROC	Receiver Operating Characteristic
RV	Random Variable
SISO	Single-Input Single-Output
SNR	Signal-to-Noise Ratio
SSR	Signal-to-Scatterer Ratio
TR	Time-Reversal

List of Symbols

$(\cdot)^{(j)}$	j-th derivative operation
$(\cdot)^*$	complex conjugate operation
$(\cdot)^\dagger$	conjugate-transpose operation
$\lvert\cdot\rvert$	matrix determinant
$\lVert\cdot\rVert$	Euclidean norm
$\langle\cdot\,,\cdot\rangle$	inner product
$\mathbf{1}(\cdot)$	indicator function
a_i	amplitude of i-th Nakagami-m channel
$c_{n,k}$	coefficient of n-th degree orthogonal polynomial
C_p	scatterer response of probing signal
C_r	scatterer response of retransmission
$\mathcal{CN}(0,1)$	standard complex Gaussian distribution
$\mathbb{C}^N$	N dimensional complex field
$\mathrm{erf}(\cdot)$	error function
E_s	energy of transmitted signal
$\mathbb{E}[\cdot]$	expectation
f_q	frequency of probing signal
$f_s(\cdot)$	approximative PDF of order s
$f_X(\cdot)$	PDF of random variable X
$F_s(\cdot)$	approximative CDF of order s
$F_X(\cdot)$	CDF of random variable X
$\widetilde{F_{\mathbf{Q}}}(\cdot)$	empirical spectral distribution of $\mathbf{Q}$
G_d	diversity gain
G_m	multiplexing gain
$\mathcal{G}_{\mathbf{Q}}(\cdot)$	Cauchy transform of $\mathbf{Q}$
$\widetilde{\mathcal{G}_{\mathbf{Q}}}(\cdot)$	resolvent of $\mathbf{Q}$
$H(\cdot\,;\cdot,\cdot)$	bivariate Hermite polynomial
H_i	scalar channel w.r.t. i-th cluster

$\mathbf{H}$	end-to-end channel matrix
$\mathbf{H}_i$	channel matrix w.r.t. i-th cluster
$\mathcal{H}_0$	null hypothesis: absence of target
$\mathcal{H}_1$	alternative hypothesis: presence of target
$I_{(\cdot)}(\cdot)$	modified Bessel function of the first kind
$\mathbf{I}_N$	$N \times N$ identity matrix
$\mathcal{I}$	mutual information
$\mathcal{I}_{\mathrm{LB}}$	lower bound of mutual information
$\mathrm{Im}(\cdot)$	imaginary part of complex number
k	energy normalization of time-reversed signal
$K_0(\cdot)$	modified Bessel function of the second kind
K_i	number of scatterers in i-th cluster
l	likelihood ratio
l_0	decision threshold
$\mathcal{L}$	linear spectral statistics
$\log\det(\cdot)$	logarithm of matrix determinant
m	parameter of Nakagami-m channel
$M_X(k)$	k-th moment of random variable X
n	number of component channels
$\mathbb{N}$	set of non-negative integers
$\mathcal{N}_n$	normalization of cascaded n channel matrices
P	amplitude of end-to-end channel
$\widetilde{P_r}(\cdot\,;\cdot)$	Cramér Edgeworth polynomial
P_c	power of scatterer response
$\mathcal{P}_K$	set of permutations of integers $1, \ldots, K$
$P_{\mathrm{out}}(\cdot)$	outage probability
$\mathrm{per}(\cdot)$	matrix permanent
Q	number of frequency samples
$\mathbf{Q}$	sample covariance matrix $\mathbf{H}\mathbf{H}^\dagger$
$\mathcal{R}(x, y)$	second order R-transform
$\mathrm{Re}(\cdot)$	real part of complex number
$\mathcal{S}_{\mathbf{Q}}$	support of limiting spectrum of $\mathbf{Q}$
T	response of point target
$\mathrm{Tr}(\cdot)$	matrix trace
$w(\cdot)$	weight function
x	transmitted signal
x_{TR}	time-reversed signal
$\mathbf{x}$	transmitted signal vector

y	received signal
y_{TR}	received signal of retransmission
$\mathbf{y}$	received signal vector
z	additive noise
$\mathbf{z}$	additive noise vector
γ	signal-to-noise ratio
$\bar{\gamma}$	average signal-to-noise ratio
γ_0	Euler's constant
$\Gamma(\cdot)$	gamma function
Δ_n	orthogonal polynomial normalization
λ_i	i-th eigenvalue of $\mathbf{Q}$
μ_X	expectation of random variable X
ν_i	i-th moment of weight function
ξ_i	i-th complex eigenvalue of $\mathbf{H}$
$\pi_n(\cdot)$	orthogonal polynomial of degree n
$\rho_{i,j}$	cross correlation between a_i^2 and a_j^2
ρ_c	cross correlation between C_p and C_r
σ_X^2	variance of random variable X
$\mathbf{\Sigma}$	covariance matrix of signal vector
$\phi_{(\cdot,\cdot)}(\cdot)$	Gaussian density function
$\Phi_{(\cdot,\cdot)}(\cdot)$	Gaussian distribution function
$\chi_{[\cdot,\cdot]}$	joint cumulants
$\psi_X(\cdot)$	characteristic function of random variable X
Ω	power of Nakagami-m fading

1. Introduction

1.1 Background

In wireless communications, the channel between transmitter and receiver operates through electromagnetic radiation. The information-bearing signals, representing texts, audios, and videos, are mapped into transmit symbols and modulated onto the carrier frequency. The radio transmission then originates from the antennas, which convert the symbols in the form of electric power to the electromagnetic waves. In realistic environment, the wave propagation may be affected by various obstacles, which causes different electromagnetic mechanisms, such as reflection, diffraction, and scattering. The induced channel variations seen by the receiver can be divided into two types:

- Large-scale fading: includes distance dependent pathloss and shadowing due to large obstructions in the main signal path. Large-scale fading takes place when the mobile equipment moves across the cellular service area, and decorrelation distance is of the order of few meters.

- Small-scale fading: results from constructive and destructive multipath fading, where the received signal is a superimposition of multiple replicas of the original signal each distorted by the corresponding path. Spatial decorrelation distance for the small-scale fading is of the order of the wavelength of the carrier frequency.

In modern cellular communications, the large-scale fading can be tackled relatively easily, e.g. by using slow transmit power control and cell planning. In this thesis, we focus on the small-scale fading and investigate the theoretical performance of the multipath fading channels.

In order to characterize the wireless channels, one can resort to solving the electromagnetic field equations. In typical cellular communication systems, the operating carrier frequency ranges from 2 GHz to 5 GHz [1, 2], where the corresponding wavelength is only a fraction of a meter. To calculate the electromagnetic field at the receiver, the location of the receiver and the structure of the physical environment should be known within sub-meter accuracy [3]. In realistic environment, the solutions of electromagnetic equations are therefore too complicated to obtain. To circumvent this difficulty, a number of multipath models have been proposed to explain the observed statistical nature of wireless fading channels [4]. These statistical models have been validated through empirical measurements in various scenarios and they serve as universal toolkits to analyze and design wireless communication systems.

The concept of cascaded fading channel was proposed as an extension on top of the basic statistical models. It aims to capture the characteristics of the channel when the signal propagates through a sequence of clusters (layers) of scatterers until it reaches the destination. As a result, the effective end-to-end channel becomes a product of component channels, each corresponding to certain cluster. In literature, the cascaded Single-Input Single-Output (SISO) Rayleigh channel is shown to model the radio propagation in urban area with moving antennas [5]. In [6, 7], authors studied the shadowing effect caused by multiple cascaded scatterers and the related physical motivation was given in [8, Sec. 3]. It is also known that the cascaded scattering channel model is useful when modeling indoor propagation [9, Chap. 13]. For transceiver equipped with multiple antennas, the cascaded Multi-Input Multi-Output (MIMO) channel, also known as the Rayleigh product channel, is useful since it captures the performance degradation due to the channel rank deficiency. This effect occurs in certain environments, where propagation is subject to the structural limits of fading channels caused by either insufficient scattering [10, 11] or the so-called keyhole effect [12]. As a result, the end-to-end MIMO channel becomes a product of channel matrices [13].

By assuming a single scatterer in each cluster, the statistics of cascaded SISO Rayleigh channels becomes comparable with a lognormal distribution as shown in [7], where the rate of convergence is quantified via numerical simulations as the number of component channels increases. Recently, the performance analysis have been also carried out for the cascaded Rayleigh [14], Nakagami-m [15] and Weibull channels [16] with

statistically independent fading components. In [14–16], the statistics of the product of Random Variables (RVs) were derived in terms of Meijer's G-functions. Furthermore, in [17] the Probability Density Function (PDF) of a product of independent Nakagami-m RVs was expressed as an infinite series by using the Mellin transform. By exploiting the properties of the Mellin transform, approximations for the statistics of products of independent Gamma, Nakagami-m and Gaussian RVs were proposed in [18].

When multiple antennas are used at the transceivers and arbitrary number of scatterers is assumed in each cluster, the performance of the cascaded MIMO channel depends on the eigenvalues of the channel matrix. In literature, the corresponding eigenvalue statistics is only known in some special cases. For the single-cluster MIMO channel, the upper bound for the ergodic capacity was derived in [12] and the exact expression was obtained in [19]. A fundamental tradeoff between the channel multiplexing gain and the diversity gain was characterized in [20]. Authors in [21, 22] investigated the asymptotic outage probability of the single-cluster MIMO channels assuming two of matrix dimensions approach infinity while the other fixed. Furthermore, in case all matrix dimensions are large, the ergodic capacity has been obtained in [11] via numerical integration. With the assumptions of [11], an asymptotic expression for the ergodic capacity was derived in [23]. In the case of two-cluster MIMO channel, the ergodic capacity was deduced in [24]. Using free probability theory, the asymptotic eigenvalue distribution was derived in [13] for the cascaded MIMO channel with arbitrary number of clusters.

1.2 Scope and objective

In this thesis, performance analysis for a wireless communication system is considered in the presence of cascaded fading channel. Essentially, the adopted multiple cluster scattering model assumes that the radio wave goes through all clusters in sequence and is bounced off from each scattering object exactly once. This assumption is valid when there is no line-of-sight between transmitter and receiver or between non-consecutive clusters. Such channel model has been also adopted in [11] and confirmed by measurement campaigns in [25, 26]. In addition, it is assumed that the receiver can track the channel and has full Channel State Information (CSI), while the transmitter has no CSI. Under these assumptions, we divide the considered cascaded fading channels into two main cate-

gories:

- In the first category, transceivers are equipped with a single antenna and there is one scattering object at each cluster. For ergodic channels, we investigate the average Signal-to-Noise Ratio (SNR) perceived by the receiver in presence of cascaded correlated Nakagami-m fading with arbitrary number of clusters. For non-ergodic channels, the outage probability is calculated. Moreover, we consider a cascaded Rician channel formed by retransmitting the backscattered signal from a point target embedded in multipath scatterings, also known as the time-reversal detection. We formulate the target detection problem as a binary hypothesis test and propose a new detection algorithm using the statistical distribution of the cascaded Rician channel.

- In the second category, transceivers are equipped with multiple antennas and there are multiple scattering objects in each cluster. The information theoretical limits, such as ergodic Mutual Information (MI) and outage probability, are obtained for ergodic and non-ergodic cascaded Rayleigh MIMO channels, respectively. By assuming that the number of scattering objects is equal to the number of antennas, the non-asymptotic lower bound for ergodic MI as well as the rate scaling law are obtained. With channel dimensions growing to infinity at fixed rate, the asymptotic outage probability is calculated for single-cluster MIMO channels. Using this result, a fundamental tradeoff between diversity and multiplexing gain is characterized at finite SNR level.

1.3 Contributions and summary of publications

This thesis consists of an introductory part and seven original publications. The content of each publication is summarized as follows.

In Publication I we derive a closed-form expression for the orthogonal polynomials with respect to the lognormal density. The obtained orthogonal polynomial is valid for a family of lognormal density functions and deemed as a more general result compared to the existing ones in literature. Using this result, an approximation for the distribution of product of RVs is derived using a moment based framework. For the product of correlated Nakagami-m RVs, numerical results show that the proposed

approximation is accurate when RVs are independent or weakly correlated.

In Publication II we utilize the results of Publication I to approximate the SNR distribution for the cascaded Nakagami-m channels with general correlation structure. We have also computed the exact average received SNR of the considered channel model.

In Publication III we consider blind time-reversal detection of a point target in the presence of correlated multipath scattering. The target detection is formulated as a binary hypothesis test, where the test statistics depends on the distribution of correlated Rician channels. To address this issue, we derive the exact characteristic function for the product of noncentral correlated complex Gaussian RVs and obtain the exact PDF when target is absent. When target is present, the PDF is shown to be asymptotically Gaussian as the means of Rician RVs go to infinity and can be approximated by the bivariate Edgeworth expansion. Simulation results show that the proposed detector outperforms the existing time-reversal detector in the presence of channel correlation.

In Publication IV we consider the cascaded MIMO channels with independent Rayleigh fading. Assuming equal number of antennas and scattering objects in each cluster, the lower bound of ergodic MI is derived by using a recent result for the eigenvalue distribution of product of complex Gaussian matrices. As the received SNR grows to infinity, a simpler expression is obtained representing the rate scaling law in the large SNR regime. This result generalizes the rate scaling law for conventional Rayleigh MIMO channels.

In Publication V we consider a single-cluster MIMO channel and derive the asymptotic variance of MI when the channel dimensions grow to infinity. As the number of antennas is equal at transmitter and receiver, we obtain an explicit expression, which can be used to compute an accurate approximation for the variance of MI over a wide range of SNRs and channel dimensions. The MI of the cascaded MIMO channel is conjectured as a Gaussian RV and the claim is validated via numerical simulations.

In Publication VI we consider the same MIMO model as in Publication V and provide a detailed proof for the asymptotic variance of the channel MI. Compared to the conventional Rayleigh MIMO channel, the increased fluctuation of MI is understood via the free probability theory. In case of large matrix dimensions, the covariance function for the eigenvalues of product matrices depends on the known free moments and the unknown

free cumulants. The latter is identified to be equivalent to the problem of counting the number of non-crossing permutations on the annulus.

In Publication VI and VII, we show that the MI of the single-cluster MIMO channel behaves asymptotically as a Gaussian RV by establishing a Central Limit Theorem (CLT) for the linear spectral statistics of matrix ensembles. Using this result, the asymptotic outage probability can be evaluated as the channel dimensions grow to infinity. This enables a simple approximation for the fundamental tradeoff between the channel diversity gain and the multiplexing gain. Numerical results show that the previously known tradeoff obtained at infinite SNR significantly overestimates diversity gain at realistic SNRs.

2. Cascaded SISO Channels

In this chapter, we consider the wireless link with single antenna at transmitter and receiver. The transmitted symbol x is conveyed from the transmitter to the receiver via n clusters in sequence, where each cluster contains one scattering object. The received symbol is then represented as

$$y = \prod_{i=1}^{n} H_i x + z, \tag{2.1}$$

where H_i denotes the channel between $(i-1)$-th and i-th clusters, and z refers to the complex Gaussian noise. To understand the performance of the equivalent end-to-end channel $\prod_{i=1}^{n} H_i$, we recall in Section 2.1 the existing moment-based approximations for the distribution of the channel statistics. The approximated distributions of channel amplitudes and the exact moments are then used to investigate the following systems:

- First, a cascaded Nakagami-m fading channel with arbitrary number of clusters is investigated in Section 2.2. The exact average end-to-end SNR and approximative outage probability are deduced.
- Second, a blind time-reversal detection is studied in Section 2.3 in the presence of a point target embedded in correlated multipath scattering. The likelihood ratio of the corresponding binary hypothesis is calculated by using the complex amplitude distribution of the time-reversed signal.

2.1 Moment-based approximation

2.1.1 Background

There are many cases where the moments of a distribution can be easily obtained, while the exact form of the distribution is intractable. In such

situations, it is convenient to utilize the moment-based approximation to estimate the unknown distribution function. Consider a RV U with unknown PDF $f_U(x)$. The moment-based approximations embrace the set of techniques to construct closed-form approximations for $f_U(x)$ using the moments of U, denoted as

$$M_U(k) = \int_a^b x^k f_U(x) \mathrm{d}x, \quad k \in \mathbb{N}, \tag{2.2}$$

where the interval $[a, b]$ is the support of PDF $f_U(x)$. For example, the approximation that uses the family of Pearson curves, as discussed in [27], utilizes up to the fourth moment of U.

Although the Pearson curves can be used to generate many simple distribution functions, they may induce non-trivial approximation error in cases where higher order moments are needed. To address this issue, the Gram-Charlier series has been proposed, see e.g. [28], where the target PDF $f_U(x)$ is expressed in terms of derivatives of a certain weight function $w(x)$, which is selected as an initial approximation to $f_U(x)$. Namely,

$$f_U(x) \approx \sum_{j=0}^{s} c_j w^{(j)}(x). \tag{2.3}$$

Applying the construction (2.3), the Gram-Charlier series can be used to match the first s moments with $f_U(x)$ [29]. The support of $w(x)$ should fit with the support of RV U, being infinite, semi-infinite, or compact set on the real axis [30]. In particular, the weight function $w(x)$ can be Gaussian, Gamma, or Beta distribution, and the corresponding derivatives $w^{(j)}(x)$ have explicit expressions in terms of Hermite, Laguerre, and Jacobi orthogonal polynomials [31]. When the RV U is a normalized sum of n i.i.d. RVs, the summation (2.3), reordered in the decreasing powers of $\sqrt{n}$, is known as the Edgeworth expansion with Gaussian density as the weight function [32]. As $n \to \infty$, the expansion (2.3) becomes asymptotic approximation for the PDF $f_U(x)$ and the approximation error can be estimated.

If the Gaussian, Gamma, and Beta distributions fail to serve as an initial approximation, other types of weight functions are needed. The Gram-Charlier series (2.3) then requires to evaluate the derivatives $w^{(j)}(x)$, where results are usually given in recursive formulas without explicit expression. To avoid this problem, authors in [33] proposed a generalized orthogonal polynomial expansion given by the product of a general weight function and non-classical orthogonal polynomials.

2.1.2 Generalized orthogonal polynomial expansion

Let $w(x)$ be a proper probability density function defined on the interval $[a, b]$, i.e. $w(x) \geq 0$ for $a \leq x \leq b$ and $\int_a^b w(x)\mathrm{d}x = 1$. We say that the n-th degree polynomial

$$\pi_n(x) = \sum_{k=0}^{n} c_{n,k} x^k \tag{2.4}$$

with $c_{n,n} \neq 0$ is orthogonal with respect to the weight function $w(x)$ if

$$\int_a^b \pi_j(x)\pi_k(x)w(x)\mathrm{d}x = \begin{cases} h_j & j = k \\ 0 & j \neq k \end{cases} \qquad j, k \in \mathbb{N}, \tag{2.5}$$

where h_j is the orthogonality factor. We denote by ν_i, $i \in \mathbb{N}$, the i-th integer moment of $w(x)$ with $\nu_i = \int_a^b x^i w(x)\mathrm{d}x$. If the moment sequence $\{\nu_i\}_{i\in\mathbb{N}}$ exists, the orthogonal polynomial $\pi_n(x)$ is monic ($c_{n,n} = 1$) and uniquely expressed by the determinant representation [34, Eq. (2.2.6)] as

$$\pi_n(x) = \frac{1}{\Delta_n} \begin{vmatrix} \nu_0 & \nu_1 & \cdots & \nu_{n-1} & \nu_n \\ \nu_1 & \nu_2 & \cdots & \nu_n & \nu_{n+1} \\ \vdots & \vdots & \ddots & \vdots & \vdots \\ \nu_{n-1} & \nu_n & \cdots & \nu_{2n-2} & \nu_{2n-1} \\ 1 & x & \cdots & x^{n-1} & x^n \end{vmatrix}, \tag{2.6}$$

where $\Delta_n = |\nu_{i+j}|_{i,j=0,\cdots,n-1}$ refers to the determinant of an $n \times n$ matrix with entry ν_{i+j} on the $(i+1)$-th row and $(j+1)$-th column, and $\Delta_0 = 1$. If $w(x)$ is properly chosen and serves as the initial approximation to the target PDF $f_U(x)$, the generalized orthogonal polynomial expansion is given by [33, Eq. (7)] such that

$$f_U(x) \approx f_s(x) = w(x) \sum_{i=0}^{s} \eta_i \pi_i(x). \tag{2.7}$$

Here, the coefficient η_i is explicitly determined by the linear equations

$$\int_a^b \pi_i(x) f_U(x)\mathrm{d}x = \int_a^b \pi_i(x) f_s(x)\mathrm{d}x, \quad i = 0, \ldots, s, \tag{2.8}$$

which equate the first s moments of $f_U(x)$ with $f_s(x)$.

Due to the orthogonality of the polynomials $\{\pi_i(x)\}$, the addition of the k-th term $w(x)\eta_k\pi_k(x)$ to the $(k-1)$-th order approximation $f_{k-1}(x)$ in (2.7) does not affect the calculation of the first k coefficients $\{\eta_i\}_{0\leq i\leq k-1}$. Therefore, the orders of approximation can be found iteratively: evaluate the maximum relative improvement of the k-th order approximation $\tau = \max_{x\in[a,b]} \|w(x)\eta_k\pi_k(x)/f_{k-1}(x)\|$. If τ is less than a pre-defined threshold τ_{TH},

use $f_k(x)$ as the approximation for $f_U(x)$, otherwise compute the $(k+1)$-th term until $\tau < \tau_{\mathrm{TH}}$ or the number of terms in approximation exceeds the maximum order $s_{\max}$.

2.1.3 Bivariate Edgeworth expansion

Consider a two-dimensional real random vector $\mathbf{U} = [U_1, U_2]$ with an unknown joint PDF $f_{\mathbf{U}}(\mathbf{u})$. If $\mathbf{U}$ is approximately Gaussian, the Edgeworth expansion [35] will be useful when calculating an approximation of the PDF $f_{\mathbf{U}}(\mathbf{u})$. Without loss of generosity, we assume that $\mathbf{U}$ has zero mean and covariance matrix $\mathbf{R}$. The characteristic function of $\mathbf{U}$ is defined as $\psi_{\mathbf{U}}(\mathbf{t}) = \mathbb{E}\left[e^{\imath\langle \mathbf{t}, \mathbf{U}\rangle}\right]$, where $\mathbf{t} = [t_1, t_2]$ is a two-dimensional real vector and $\langle \cdot, \cdot \rangle$ refers to the inner product of vectors. Consider the cumulant generating function $\log\left(\psi_{\mathbf{U}}(\mathbf{t})\right)$ expanded around $\mathbf{t} = [0, 0]$ such that

$$\log\left(\psi_{\mathbf{U}}(\mathbf{t})\right) = -\frac{1}{2}\langle \mathbf{t}, \mathbf{R}\,\mathbf{t}\rangle + \sum_{r=1}^{s} \chi_{r+2}(\imath\,\mathbf{t}) + \mathcal{O}(\|\mathbf{t}\|^s). \tag{2.9}$$

The bivariate polynomial $\chi_s(\cdot)$ is expressed by [35, Eq. (7.1)] as

$$\chi_s(\mathbf{t}) = \sum_{\kappa_1+\kappa_2=s} \frac{\chi_{[\kappa_1,\kappa_2]}}{\kappa_1!\kappa_2!} t_1^{\kappa_1} t_2^{\kappa_2}, \tag{2.10}$$

where $\chi_{[\kappa_1,\kappa_2]}$ refers to the mixed cumulant of RVs U_1 and U_2 and the summation is taken over $\kappa_1+\kappa_2 = s$ with $\kappa_1, \kappa_2 \in \mathbb{N}$. By using the mapping between cumulants and moments of multivariate distribution [36], $\chi_{[\kappa_1,\kappa_2]}$ can be calculated as a linear combination of the mixed moments $\mathbb{E}\left[U_1^i U_2^j\right]$, $0 \le i \le \kappa_1, 0 \le j \le \kappa_2$. Taking the exponential on both sides of (2.9) and expanding around $\mathbf{t} = [0, 0]$, an approximation for the characteristic function $\psi_{\mathbf{U}}(\cdot)$ was obtained in [37] as

$$\psi_{\mathbf{U}}(\mathbf{t}) \approx \psi_s(\mathbf{t}) = \exp\left(-\frac{1}{2}\langle \mathbf{t}, \mathbf{R}\,\mathbf{t}\rangle\right)\left[1 + \sum_{r=1}^{s-2} \widetilde{P_r}\left(\imath\,\mathbf{t}; \{\chi_{\kappa_1,\kappa_2}\}\right)\right], \tag{2.11}$$

where $\widetilde{P_r}\left(\imath\,\mathbf{t}; \{\chi_{\kappa_1,\kappa_2}\}\right)$ refers to the bivariate Cramér Edgeworth polynomial in $\imath\,\mathbf{t}$ depending on $\chi_3, \ldots, \chi_{r+2}$. An explicit formula of $\widetilde{P_r}$ can be found in [35, Eq. (7.3)]. By the inverse transform of (2.11), the Edgeworth approximation for the PDF $f_{\mathbf{U}}(\mathbf{u})$ is given as

$$f_{\mathbf{U}}(\mathbf{u}) \approx f_s(\mathbf{u}) = \frac{1}{2\pi}\int \psi_s(\mathbf{t}) \exp\left(-\imath\langle \mathbf{t}, \mathbf{u}\rangle\right) \mathrm{d}\mathbf{t}, \tag{2.12}$$

where $\mathbf{u} = [u_1, u_2]$ and $\mathrm{d}\mathbf{t} = \mathrm{d}t_1\mathrm{d}t_2$. Using the properties of Fourier transform, the integral in (2.12) can be explicitly expressed as

$$f_s(\mathbf{u}) = \phi_{0,\mathbf{R}}(\mathbf{u}) + \sum_{r=1}^{s-2} P_r\left(\phi_{0,\mathbf{R}}(\mathbf{u}); \{\chi_{[\kappa_1,\kappa_2]}\}\right), \tag{2.13}$$

where $\phi_{0,\mathbf{R}}$ denotes a bivariate Gaussian density function with zero mean and covariance matrix $\mathbf{R}$. According to [35, Lemma 7.2], P_r is formed by substituting each $t_1^{\kappa_1}t_2^{\kappa_2}$ in expression of $\widetilde{P_r}$ with $H(\mathbf{u};[\kappa_1,\kappa_2],\mathbf{R}^{-1})\phi_{0,\mathbf{R}}(\mathbf{u})$ where H is the bivariate Hermite polynomial [38].

2.2 Cascaded Nakagami-m channels

2.2.1 Signal model

Consider a cascaded Nakagami-m communication channel (2.1) with complex Gaussian noise $z \sim \mathcal{CN}(0,\sigma_z^2)$ and component channel $H_i = a_i e^{\imath\phi_i}$, $i = 1,\ldots,n$. Here, amplitudes $\{a_i\}_{1\le i\le n}$ are jointly Nakagami-m distributed with the PDF given by [39] as

$$f(a_1,a_2,\cdots,a_n) = \int_0^\infty \frac{t^{m-1}}{\Gamma(m)}\exp(-t)\prod_{i=1}^{n}\frac{1}{(\beta_i^2\rho_i^2\,t)^{\frac{m-1}{2}}}\frac{a_i^m}{\omega_i^2} \times \exp\left(-\frac{a_i^2+\beta_i^2\rho_i^2\,t}{2\omega_i^2}\right) I_{m-1}\left(\frac{a_i\sqrt{\beta_i^2\rho_i^2\,t}}{\omega_i^2}\right)\mathrm{d}t, \quad (2.14)$$

where $\beta_i^2 = \Omega_i/m$, $\omega_i^2 = \beta_i^2\left(1-\rho_i^2\right)/2$ and $I_{m-1}(\cdot)$ refers to the modified Bessel function of the first kind [40, Eq. (8.406)]. The parameter $m \ge 1/2$ represents the severity of fading and takes integer or half-integer values in (2.14). The power of the component channel H_i is denoted by $\mathbb{E}[a_i^2] = \Omega_i$ and the cross-correlation between a_i^2 and a_j^2 is of the form

$$\rho_{i,j} = \frac{\mathbb{E}[a_i^2a_j^2] - \mathbb{E}[a_i^2]\mathbb{E}[a_j^2]}{\sqrt{\mathrm{Var}[a_i^2]\mathrm{Var}[a_j^2]}} = \rho_i^2\rho_j^2, \quad (2.15)$$

where $-1 \le \rho_i, \rho_j \le 1$. We denote by P the end-to-end amplitude of the cascaded channel, i.e.

$$P = \prod_{i=1}^{n} a_i. \quad (2.16)$$

Then the instantaneous SNR of the cascaded channel (2.1) reads

$$\gamma = \frac{E_s}{\sigma_z^2}P^2, \quad (2.17)$$

where $E_s = \mathbb{E}[\|x\|^2]$ refers to the average energy of the transmitted symbol.

2.2.2 Product of Nakagami-m random variables

Using the orthogonal polynomial expansion described in Section 2.1.2, the distribution of the product of amplitudes P in (2.16) can be obtained. In

light of the CLT for product of RVs, the lognormal density $f_{\mathrm{LN}}(x)$ is chosen as the weight function $w(x)$ in the expansion (2.7),

$$f_{\mathrm{LN}}(x) = \frac{1}{x\sqrt{2\pi\sigma_w^2}} \exp\left(-\frac{(\log x - \mu_w)^2}{2\sigma_w^2}\right), \quad x \in (0, \infty). \tag{2.18}$$

In Publication I, the orthogonal polynomial $\pi_n(x) = \sum_{k=0}^{n} c_{n,k} x^k$ with respect to the lognormal density $f_{\mathrm{LN}}(x)$ was derived. The resulting polynomial coefficients $c_{n,k}$ are given by

$$c_{n,k} = (-1)^{n+k} e^{(n-k)\mu_w} q^{(n-1/2)(n-k)} \begin{bmatrix} n \\ k \end{bmatrix}_q, \tag{2.19}$$

where $q = e^{\sigma_w^2}$ and the generalized binomial coefficient is of the form

$$\begin{bmatrix} n \\ k \end{bmatrix}_q = \frac{(1-q^n)(1-q^{n-1})\cdots(1-q^{n-k+1})}{(1-q^k)(1-q^{k-1})\cdots(1-q)}. \tag{2.20}$$

With $w(x) = f_{\mathrm{LN}}(x)$, the coefficient η_i in (2.7) is obtained by solving the linear system (2.8) as

$$\eta_i = \frac{1}{h_i} \sum_{k=0}^{i} c_{i,k} M_P(k), \tag{2.21}$$

where $M_P(k) = \mathbb{E}\left[P^k\right]$ is the k-th moment of the end-to-end channel amplitude P. Using the joint PDF (2.14), $M_P(k)$ can be calculated by integrating $P^k = \left(\prod_{i=1}^{n} a_i\right)^k$ over the measure $f(a_1, \ldots, a_n)\mathrm{d}a_1 \ldots \mathrm{d}a_n$. The parameters μ_w and σ_w^2 of the lognormal density $f_{\mathrm{LN}}(x)$ are set equal with the mean and variance of $\log(P)$, respectively. Detailed derivations of $M_P(k)$, μ_w, and σ_w^2 are given in Publication II.

By rearranging the terms of the expansion (2.7), the approximation $f_s(x)$ can be rewritten as a product of the lognormal density $f_{\mathrm{LN}}(x)$ and a polynomial $\sum_{i=0}^{s} \varpi_i x^i$, where $\varpi_j = \sum_{k=j}^{s} c_{k,j}\eta_k$. After direct integration, the approximation for the Cumulative Distribution Function (CDF) of P attains the form

$$F_s(x) = \sum_{i=0}^{s} \varpi_i \nu_i \Phi_{0,1}\left(\frac{\log(x) - \mu_w}{\sigma_w} - i\sigma_w\right), \tag{2.22}$$

where $\nu_i = \exp\left(i\mu_w + i^2\sigma_w^2/2\right)$ is the i-th moment of $f_{\mathrm{LN}}(x)$, $\Phi_{0,1}(x) = \left(1 + \mathrm{erf}(x/\sqrt{2})\right)/2$ is the CDF of a standard Gaussian RV, and $\mathrm{erf}(\cdot)$ refers to the error function.

2.2.3 Numerical results

Let us evaluate numerically the average end-to-end SNR and the SNR distribution for the cascaded Nakagami-m channel. First, we consider the average SNR $\bar{\gamma} = \mathbb{E}[\gamma]$ such that

$$\bar{\gamma} = \frac{E_s}{\sigma_z^2}\mathbb{E}\left[P^2\right] = \frac{E_s}{\sigma_z^2} M_P(2). \tag{2.23}$$

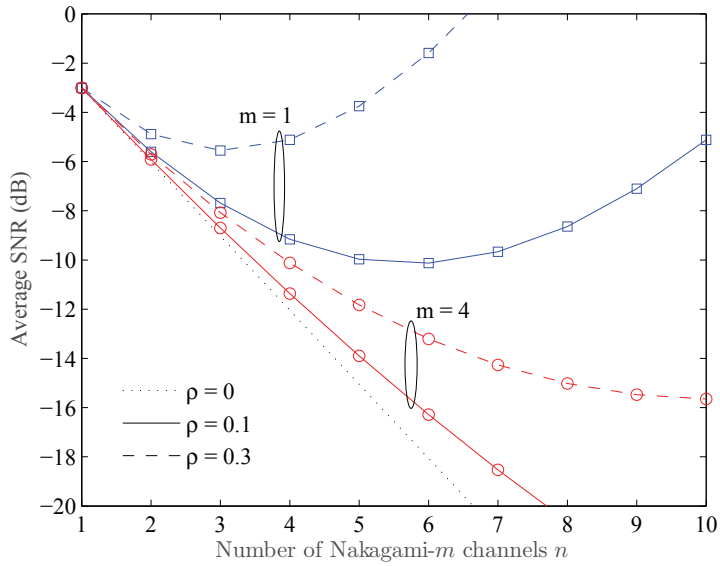

Figure 2.1. Average end-to-end SNR of cascaded Nakagami-m channel as a function of the number of component channels n with $\Omega = 0.5$. Dotted line: $\rho = 0$; solid line: $\rho = 0.1$; dashed line: $\rho = 0.3$.

In Fig. 2.1, $\bar{\gamma}$ is plotted as a function of the number of component channels n, for $\rho_i = \rho = 0$ (independent), 0.1 and 0.3, $i = 1 \ldots, n$. The same power $\Omega = \Omega_i = 0.5$ is used for all component channels and the constant E_s/σ_z^2 is set to be 1. From Fig. 2.1, we find that the average SNR is larger in the presence of channel correlation compared with the independent case. Furthermore, as the number of channels increases, the amount of improvement in average SNR also increases, especially when $m = 1$. The obtained results also indicate that with certain parameter combinations (e.g. $m = 1$, $n = 6$, and $\rho = 0.3$), the cascaded fading channels achieve better average SNRs than a single Nakagami-m channel ($n = 1$).

Next, we consider the outage probability $P_{\text{out}}(x)$ of the cascaded channel defined as the probability that the instantaneous SNR γ falls below a given threshold x. By utilizing the CDF of the end-to-end amplitude P in (2.22), $P_{\text{out}}(x)$ can be obtained as

$$P_{\text{out}}(x) \approx F_s\left(\sqrt{\frac{\sigma_z^2}{E_s}x}\right). \tag{2.24}$$

In Fig. 2.2, the outage probabilities of the cascaded Nakagami-m channel are plotted as a function of the end-to-end SNR. The component channels are assumed to be identically distributed with parameters $m = 4$, $\Omega = 0.8$ and equal cross-correlation with values $\rho = 0.1$ and 0.3. The approxima-

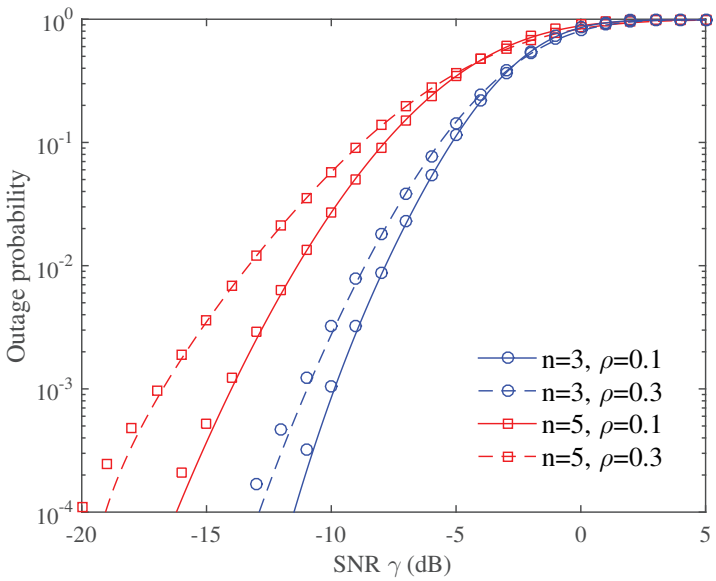

Figure 2.2. Outage probability as a function of the SNR for cascaded Nakagami-m channels with $m = 4$ and $\Omega = 0.8$. Solid line: $\rho = 0.1$; dashed line: $\rho = 0.3$. Simulated values are denoted by markers.

tive outage probability (2.24) is evaluated for 3 and 5 clusters of cascaded channels, and numerical simulations are used to validate approximations.

2.3 Cascaded Rician channels and blind time-reversal detection

In this section, we consider a cascaded channel with two Rician fading components. This channel is useful when modeling the so-called Time-Reversal (TR) transmission in the electromagnetic field. The TR technique utilizes channel reciprocity and obtains the channel state information by sending a probing signal. The backscattered signal is then time-reversed and retransmitted. The TR signal is shown to be optimal in the sense that the transmission system realizes a matched filter to the propagation transfer function [41]. In [42–45], authors have introduced the TR detection in the wireless multipath environment.

2.3.1 Time-reversal detection

We consider the blind detection of a point target embedded in the multipath scattering similarly as in [45]. The detection system sends Q probing signals at the frequencies f_q, $q \in [1,\ Q]$. The sampling frequencies are

chosen such that the frequency bins are separated by the channel coherence bandwidth and the spectral samples are statistically independent. The multipath channel induced by the scattering is modeled as a wide sense stationary process. We denote by $C_p(q)$ and $C_r(q)$ the channels experienced by the probing signal and the retransmission at frequency f_q, respectively. The point target to be detected is modeled as a deterministic response T and the probing signal at f_q is denoted as $x(q)$.

After transmitting the probing signal $x(q)$, the backscattered signal is given by [45, Eq. (36)] as

$$y(q) = \big(T + C_p(q)\big)x(q) + z_p(q), \quad q = 1, \dots, Q,$$

where $z_p(q)$ is the measurement noise distributed as a zero-mean complex Gaussian RV, i.e. $z_p(q) \sim \mathcal{CN}(0, \sigma_z^2)$. In the following, we assume that the total transmit power E_s is equally allocated to the Q samples, such that $x(q) = \sqrt{E_s/Q}$. The received signal $y(q)$ is then time-reversed or, equivalently, phase-conjugated in the frequency domain and scaled to obtain the TR signal:

$$x_{\mathrm{TR}}(q) = k y(q)^{\dagger}, \tag{2.25}$$

where k is a constant energy normalization. The TR signal $x_{\mathrm{TR}}(q)$ is subsequently transmitted and the response of the retransmission is given by

$$\begin{aligned} y_{\mathrm{TR}}(q) &= \big(T + C_r(q)\big)x_{\mathrm{TR}}(q) + z_r(q) \\ &= H_2(q)H_1(q) + z_r(q), \end{aligned} \tag{2.26}$$

where $H_2(q) = T + C_r(q)$, $H_1(q) = x_{\mathrm{TR}}(q)$ and $z_r(q) \sim \mathcal{CN}(0, \sigma_z^2)$ is the measurement noise of the retransmission.

In blind TR detection, the channels $C_p(q)$ and $C_r(q)$ will not be estimated by the detector and are known only through their statistical distributions. We assume that $C_p(q)$ and $C_r(q)$ admit a bivariate zero-mean complex Gaussian distribution with a common Power Spectral Density (PSD) $P_c(q)$ and correlation coefficient $\rho_c(q)$. The measurement noises $z_p(q)$ and $z_r(q)$ are independent of each other and independent of the multipath channels. Therefore, the model (2.26) resembles a cascaded Rician channel with two fading components such that

$$H_1(q) \sim \mathcal{CN}\left(k\,T^*\sqrt{E_s/Q}, k^2\left(P_c(q)E_s/Q + \sigma_z^2\right)\right), \tag{2.27}$$

$$H_2(q) \sim \mathcal{CN}\big(T, P_c(q)\big). \tag{2.28}$$

By definition, $H_1(q)$ and $H_2(q)$ are jointly complex Gaussian distributed

with a correlation coefficient calculated as

$$\rho(q) = \frac{\mathbb{E}[(H_1(q) - \mu_1)(H_2(q) - \mu_2)^*]}{\sigma_1 \sigma_2} = \frac{\rho_c(q)^*}{\sqrt{1 + \sigma_z^2 Q / P_c(q) E_s}}, \tag{2.29}$$

where μ_i and σ_i, $i \in \{1, 2\}$, refer to the mean and variance of the RV $H_i(q)$.

If we ignore the noise term $z_r(q)$ in (2.26), $y_{\mathrm{TR}}(q)$ is a product of two non-central complex Gaussian RVs, hereafter denoted by

$$P(q) = H_2(q) H_1(q). \tag{2.30}$$

Using $P(q)$, we set up a binary hypothesis test, related to the presence or absence of the deterministic point target T. In the null hypothesis $\mathcal{H}_0$, the target is not present and $T = 0$; in the alternative hypothesis $\mathcal{H}_1$, $\|T\| > 0$. Thus,

$$\begin{aligned} \mathcal{H}_0 : &\quad \mu_1 = 0, \quad \mu_2 = 0 \\ \mathcal{H}_1 : &\quad \mu_1 = T, \quad \mu_2 = k\, T^* \sqrt{E_s / Q}. \end{aligned} \tag{2.31}$$

The PDF of $P(q)$ in the complex plane is denoted as $f_{P(q)}(p_1, p_2; T)$, where $p_1 = \mathrm{Re}\big(P(q)\big)$ and $p_2 = \mathrm{Im}\big(P(q)\big)$ are real and imaginary parts of $P(q)$. The Likelihood Ratio Test (LRT) of the blind TR detection (2.31) is constructed as

$$l = \prod_{q=1}^{Q} \frac{f_{P(q)}(p_1, p_2; T)}{f_{P(q)}(p_1, p_2; 0)} \underset{\mathcal{H}_0}{\overset{\mathcal{H}_1}{\gtrless}} l_0, \tag{2.32}$$

with l_0 being a decision threshold.

2.3.2 Product of non-central complex Gaussian random variables

Let us present the results for the exact expression of the PDF $f_{P(q)}(p_1, p_2; 0)$ obtained from the characteristic function of $P(q)$ and an approximative expression of $f_{P(q)}(p_1, p_2; T)$ while applying the bivariate Edgeworth expansion described in Section 2.1.3. The frequency index q is omitted hereafter whenever it is clear from the context.

Under the null hypothesis $\mathcal{H}_0$, the PDF of TR signal P is derived in Publication III as

$$f_P(p_1, p_2; 0) = \frac{2}{\pi \sigma_1 \sigma_2 c} \exp\left\{ \frac{2\mathrm{Re}[\rho^* p]}{c} \right\} K_0\left(\frac{2\|p\|}{c} \right), \tag{2.33}$$

where $p = p_1 + \imath p_2$, $c = \sigma_1 \sigma_2 (1 - \|\rho\|^2)$, and $K_0(x)$ is the modified Bessel function of the second kind [40, eq. (8.432/6)]. The PDF (2.33) is obtained by applying the inverse Fourier transform of the characteristic function

$\psi_P(t)$ of the complex RV P. With non-zero μ_1 and μ_2, the characteristic function $\psi_P(t) = \mathbb{E}[\exp(\imath \mathrm{Re}[t^* P])]$ is calculated in Publication III as

$$\psi_P(t) = \frac{1}{G(t)} \exp\left(-\frac{\|\mu_1\|^2\sigma_2^2 + \|\mu_2\|^2\sigma_1^2}{4G(t)}\|t\|^2 + \frac{\sigma_1\sigma_2 \mathrm{Re}[{\mu_1}^*\mu_2\rho]}{2G(t)}\|t\|^2 + \frac{\imath \mathrm{Re}[{\mu_1}^*\mu_2 t]}{G(t)} \right), \tag{2.34}$$

where $G(t) = 1 + \sigma_1^2\sigma_2^2(1 - \|\rho\|^2)\|t\|^2/4 - \imath\sigma_1\sigma_2\mathrm{Re}[t^*\rho]$.

Let $\mu_P = \mu_1{\mu_2}^* + \rho\sigma_1\sigma_2$ and $\sigma_P^2 = \|\mu_1\|^2\sigma_2^2 + \|\mu_2\|^2\sigma_1^2 + \sigma_1^2\sigma_2^2$. Then the characteristic function of $(P - \mu_P)/\sigma_P$ reads

$$\exp\left(-\imath \frac{\mathrm{Re}\left[\mu_P t^*\right]}{\sigma_P}\right) \psi_P\left(\frac{t}{\sigma_P}\right). \tag{2.35}$$

By letting $\|\mu_1/\sigma_1\|$ and $\|\mu_2/\sigma_2\|$ go to infinity, (2.35) reduces to $\exp(-\|t\|^2/4)$, which is the characteristic function of the standard complex Gaussian RV. Thus, the RV P is approximately complex Gaussian with mean μ_P and variance σ_P^2. Using the bivariate Edgeworth expansion (2.13), an approximative PDF $f_P(p_1, p_2; T)$ under alternative hypothesis $\mathcal{H}_1$ can be obtained. The exact moments of P, which are needed in approximation (2.13), are computed in Publication III.

2.3.3 Numerical results

We consider a scenario where the point target has a constant response $T = e^{\imath\pi/4}$ and the multipath channels are of equal PSD, $P_c(q) = P_c$, and equal channel correlation, $\rho_c(q) = \rho_c$, over the frequency bands $\{f_q\}_{1\le q\le Q}$. This assumption can be justified using Jakes' fading model with high-frequency samples. The Signal-to-Scatterer Ratio (SSR) and SNR are defined as $\mathrm{SSR} = 10\log_{10}\left(\|T\|^2/P_c\right)$ and $\mathrm{SNR} = 10\log_{10}\left(E_s\|T\|^2/(Q\sigma_z^2)\right)$ with $E_s = 1$. The performance of the proposed LRT detector (2.32) under channel correlation, denoted as LRT-C, is evaluated with randomly selected correlation coefficients $\rho_c = 0.1 + 0.4\imath$ and $\rho_c = 0.1 + 0.7\imath$, representing weakly correlated and strongly correlated channels. In addition, we consider the case where the target has a relatively strong channel response ($\mathrm{SSR} = 5$ dB, $\mathrm{SNR} = 5$ dB) with sample size $Q = 5$, denoted by the square markers in Fig. 2.3, and relatively weak target response ($\mathrm{SSR} = 0$ dB, $\mathrm{SNR} = 0$ dB) with $Q = 20$, denoted by the circle markers.

Fig. 2.3 shows results from Monte Carlo simulations for the Receiver Operating Characteristic (ROC), where the detection probability (Pd) is plotted as a function of the false alarm probability (Pfa). The ROC of the proposed LRT-C detector is evaluated by test (2.32). For comparison purposes, we have also computed the ROCs of the LRT detector designed for

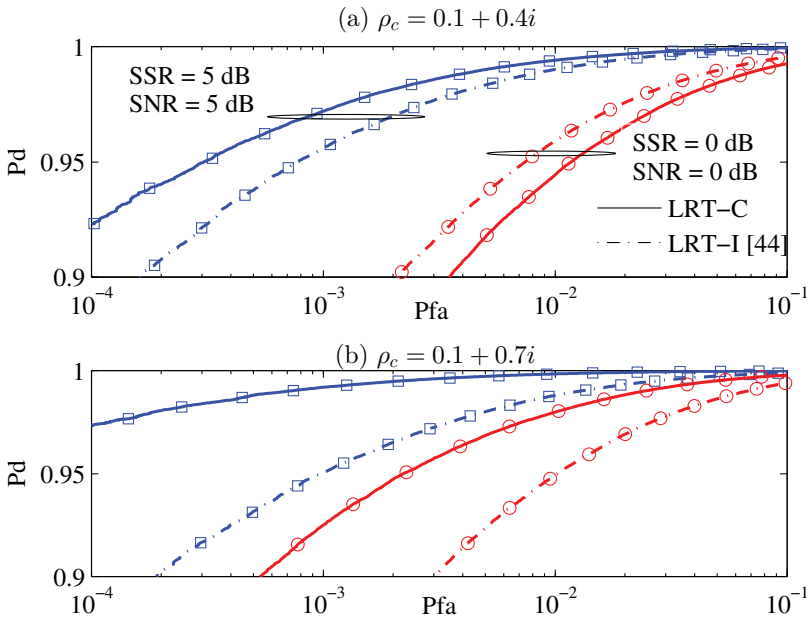

Figure 2.3. Receiver operating characteristic for the proposed LRT-C (2.32) and LRT-I of [45] for relatively strong target signal (SSR $= 5$ dB, SNR $= 5$ dB) with sample size $Q = 5$, denoted by '$\square$'; and relatively weak target signal (SSR $=$ 0 dB, SNR $= 0$ dB) with sample size $Q = 20$, denoted by '$\bigcirc$'. (a) $\rho_c = 0.1+0.4i$ and (b) $\rho_c = 0.1 + 0.7i$.

independent TR channels (LRT-I) [45]. From Fig. 2.3 we observe that the proposed LRT-C detector outperforms the existing LRT-I by a substantial margin when the target is relatively strong. These results are expected, since the LRT-C detector utilizes the channel correlation, which increases the extent of coherence between the TR signal and the multipath channel. As ρ_c increases to $0.1 + 0.7i$, the blind TR detection approaches a coherent detection, and the proposed LRT-C detector attains improved detection probability at a fixed false alarm probability by capturing the channel correlation. When the target response is weak and channel correlation is small, the performance of LRT-C becomes worse than the performance of LRT-I. This observation is consistent with the Neyman-Pearson theorem [46], as $f_P(p_1, p_2; T)$ is dominantly affected by the singularity point at origin under the condition of a weak target and small channel correlation. In this case, the approximation error of (2.13) leads to a non-trivial deviation from the optimal detector.

3. Cascaded MIMO Rayleigh Channels

The cascaded SISO channel model discussed in Chapter 2 can be naturally extended to MIMO channel by assuming multiple antennas and multiple scattering objects in each cluster. If amplitudes of all component MIMO channels are following Rayleigh fading, this model is known as the Rayleigh product channel in literature (as in [20], [47], and [48], among others). The information theoretical quantities of MIMO channel, such as ergodic mutual information and outage probability, depend on the statistics of eigenvalues of related channel matrices. In the following discussion, we first present the system model and physical motivation for the Rayleigh product channels in Section 3.1. In Section 3.2, the MIMO mutual information is formulated as the linear spectral statistics of the Rayleigh product ensembles and key mathematical results are outlined. Based on these results, closed form expressions for the lower bound of ergodic MI and for the asymptotic outage probability are given in Section 3.3, where analytical results are also illustrated and validated through simulations.

3.1 System model

3.1.1 Channel model

Consider a discrete-time, baseband MIMO system with K_0 transmit and K_n receive antennas. Information symbols are conveyed from the transmitter to the receiver via $n-1$ successive clusters of scatterers, where the i-th cluster has K_i scatterers as shown in Fig. 3.1. The end-to-end equivalent channel matrix $\mathbf{H}$ is given by

$$\mathbf{H} = \frac{1}{\sqrt{\mathcal{N}_n}} \mathbf{H}_n \cdots \mathbf{H}_1, \tag{3.1}$$

where the MIMO channels between the $(i-1)$-th cluster and i-th cluster are denoted by $\mathbf{H}_i$. We assume that the component channels $\mathbf{H}_i$, $1 \leq i \leq n$, are flat fading and follow i.i.d. complex Gaussian distribution with zero mean and unit variance. The channels corresponding to different clusters are statistically independent of each other. In line with [11, 13], the channel matrix $\mathbf{H}$ is normalized by the constant $\mathcal{N}_n = \prod_{i=1}^{n} K_i$ so that the total energy of the channel is equal to an AWGN channel with an array gain $\mathbb{E}[\mathrm{Tr}(\mathbf{H}\mathbf{H}^{\dagger})] = \sum_{i,j} \mathbb{E}[\|H_{ij}\|^2] = K_0$.

The presence of independent Gaussian matrix $\mathbf{H}_i$ in (3.1) requires independent and richly-scattered environment between the $(i-1)$-th and i-th clusters, where a large number of independently reflected and scattered paths exists [3]. Between the channels $\mathbf{H}_i$ and $\mathbf{H}_{i+1}$, the two environments are connected only via the K_i scatterers/keyholes. By using different numbers of clusters and scatterers, the cascaded MIMO channel (3.1) embraces a general family of MIMO fading channels. For instance, when $n = 1$ it corresponds to the conventional Rayleigh MIMO channel [49]. And when $n = 2$ and $K_1 = 1$, it degenerates into the MIMO keyhole channel [12]. In [10, 11], the channel (3.1) is known as double scattering channel[1] when $n = 2$ and K_1 is arbitrary. In [25], this MIMO model was validated by a measurement campaign in a typical office building. For cascaded MIMO model with arbitrary number of clusters, the asymptotic eigenvalue distribution of the channel matrix was studied in [13]. Note that the channel model (3.1) has been also used to described the multi-hop MIMO relay channels assuming noiseless relays [50, 51].

3.1.2 Signal model and mutual information

The channel output vector $\mathbf{y} \in \mathbb{C}^{K_n}$ at a given time instance is of the form

$$\mathbf{y} = \mathbf{H}\mathbf{x} + \mathbf{z}, \tag{3.2}$$

where $\mathbf{x} \in \mathbb{C}^{K_0}$ is the transmit vector that follows the complex Gaussian distribution $\mathbf{x} \sim \mathcal{CN}(\mathbf{0}, \mathbf{\Sigma})$ with $\mathbf{\Sigma} = \mathbb{E}[\mathbf{x}\mathbf{x}^{\dagger}]$. The additive noise $\mathbf{z} \in \mathbb{C}^{K_n}$ is modeled as an i.i.d. complex Gaussian vector, i.e. $\mathbf{z} \sim \mathcal{CN}(\mathbf{0}, \mathbf{I}_{K_n})$.

As the channel $\mathbf{H}$ is only known at the receiver but not at the transmit-

[1] A more general MIMO model is considered in [10, 11]. The channel is characterized by a matrix product involving three deterministic matrices, i.e. transmit, receive, and scatterer correlation matrices, and two independent complex Gaussian matrices. As a special case, the channel (3.1) corresponds to the scenario where the antenna elements and the scattering objects are sufficiently separated that the spatial correlations can be ignored.

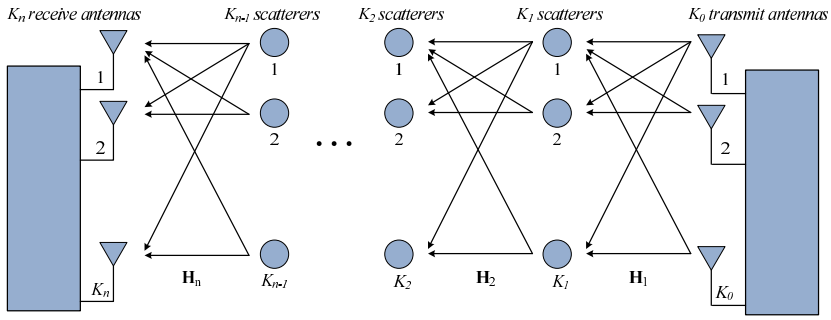

Figure 3.1. MIMO communications over the Rayleigh product channel with K_0 transmit antennas, K_n receive antennas, and K_i scatterers in i-th cluster.

ter, the transmit symbols are independent across antennas and the power is equally allocated, i.e. $\mathbf{\Sigma} = \bar{\gamma}\mathbf{I}_{K_0}$. Here, $\bar{\gamma}$ refers to the average SNR per received antenna. The instantaneous MI of the MIMO channel (3.2) in nats/sec/Hz is given by [11, Eq. (51)] as

$$\mathcal{I} = \log\det\left(\mathbf{I}_{K_n} + \bar{\gamma}\mathbf{H}\mathbf{H}^\dagger\right). \tag{3.3}$$

By eigenvalue decomposition, the Hermitian matrix $\mathbf{Q} = \mathbf{H}\mathbf{H}^\dagger$ can be written as $\mathbf{U}\mathbf{\Lambda}\mathbf{U}^\dagger$, where $\mathbf{\Lambda}$ is a diagonal matrix with entries $\mathbf{\Lambda}_{i,i} = \lambda_i$ being the ordered eigenvalues of $\mathbf{Q}$. The matrix $\mathbf{U}$ is unitary with the i-th column being the eigenvector corresponding to λ_i. Substituting the matrix decomposition into (3.3), $\mathcal{I}$ can be written in terms of λ_i as

$$\mathcal{I} = \sum_{i=1}^{K_n} \log\left(1 + \bar{\gamma}\,\lambda_i\right). \tag{3.4}$$

For the forthcoming analysis, we introduce the Empirical Spectral Distribution (ESD) of the Hermitian matrix $\mathbf{Q}$ as

$$\widetilde{F_{\mathbf{Q}}}(\lambda) = \frac{1}{K_n}\sum_{i=1}^{K_n} \mathbf{1}(\lambda_i \le \lambda),$$

where $\mathbf{1}(\cdot)$ denotes the indicator function. Now the MI (3.4) can be rewritten in terms of $\widetilde{F_{\mathbf{Q}}}(\lambda)$ as

$$\mathcal{I} = K_n \int \log(1 + \bar{\gamma}\,\lambda)\,\mathrm{d}\widetilde{F_{\mathbf{Q}}}(\lambda). \tag{3.5}$$

3.2 Linear spectral statistics of Rayleigh product ensembles

The normalized statistic $\mathcal{I}/K_n$ is known as the Linear Spectral Statistics (LSS) of random matrix $\mathbf{Q}$ [52]. For a general function $\varphi(\cdot)$, we obtain

explicit expressions for the mean and distribution of the statistic

$$\mathcal{L} = \frac{1}{K_n} \sum_{i=1}^{K_n} \varphi(\lambda_i) = \int \varphi(\lambda) \, \mathrm{d}\widetilde{F_{\mathbf{Q}}}(\lambda). \tag{3.6}$$

These results are divided into non-asymptotic one for finite dimensional matrix $\mathbf{Q}$ and asymptotic one with dimensions of $\mathbf{Q}$ growing to infinity.

3.2.1 Non-asymptotic ergodic statistics

Evaluating the ergodic LSS $\mathbb{E}[\mathcal{L}]$ of finite dimensional matrix $\mathbf{Q}$ requires the joint density of the eigenvalues of $\mathbf{Q}$. Upon the submission of Publication IV, there was no computable closed-form expression for the finite dimensional Rayleigh product ensembles with arbitrary n. By assuming that all matrix dimensions are identical, i.e. $K_i = K$, $0 \leq i \leq n$, a lower bound for the ergodic LSS becomes available. This lower bound is enabled by the Weyl's inequality between the real eigenvalue of $\mathbf{Q}$ and the complex eigenvalues of matrix $\mathbf{H}$, the joint density of which is recently derived in [53].

By eigenvalue decomposition, the square matrix $\mathbf{H}$ can be factorized as $\mathbf{H} = \mathbf{V}\mathbf{\Xi}\mathbf{V}^{-1}$, where $\mathbf{\Xi}$ is a diagonal matrix. The diagonal entries $\mathbf{\Xi}_{i,i} = \xi_i$ are the complex eigenvalues of $\mathbf{H}$ with ordered squared absolute values, i.e. $0 \leq \|\xi_K\|^2 \leq \cdots \leq \|\xi_1\|^2 < \infty$. The partial LSS of matrix $\mathbf{Q}$ is lower bounded by the Weyl's inequality [54]

$$\sum_{i=1}^{m} \varphi(\lambda_i) \geq \sum_{i=1}^{m} \varphi(\|\xi_i\|^2), \quad \forall m \in \{1, \ldots, K\}, \tag{3.7}$$

where the function $\varphi(t)$ is assumed to satisfy the following conditions:

1. $\varphi(t)$ is an increasing function for $t > 0$;
2. $\varphi(e^t)$ is a convex function of t;
3. $\varphi(0) = \lim_{t \to 0} \varphi(t) = 0$.

According to [53], the joint density of squared absolute values $y_i = \mathcal{N}_n \|\xi_i\|^2$, $i = 1, \ldots, K$, is given by

$$f(y_1, \ldots, y_K) = \mathrm{per}\left(\frac{y_i^{j-1}}{\Gamma(j)^n} g_n\left(\sqrt{y_i}\right) \right), \quad 0 \leq y_K \leq \cdots \leq y_1 < \infty, \tag{3.8}$$

where the argument of the operator $\mathrm{per}(\cdot)$ is a $K \times K$ matrix, i.e. $i, j = 1, \ldots, K$. The operator $\mathrm{per}(\mathbf{A})$ denotes the permanent of matrix $\mathbf{A} = (a_{i,j})$ such that

$$\mathrm{per}(\mathbf{A}) = \sum_{\sigma \in \mathcal{P}_K} \prod_{i=1}^{K} a_{i,\sigma(i)}, \tag{3.9}$$

where $\sigma = \{\sigma(i)\}_{1\leq i\leq K}$ is a permutation of the integers $1,\ldots,K$, and the sum is taken over all the $K!$ permutations $\mathcal{P}_K$. In (3.8), the function

$$g_n\left(\sqrt{y_i}\right) = G_{0,n}^{n,0}\left(y_i \left| \begin{matrix} - \\ 0,\ldots,0 \end{matrix} \right.\right) \tag{3.10}$$

refers to the Meijer's G-function. The general form of G-function is given by

$$G_{p,q}^{m,n}\left(x \left| \begin{matrix} a_1,\ldots,a_n,a_{n+1},\ldots,a_p \\ b_1,\ldots,b_m,b_{m+1},\ldots,b_q \end{matrix} \right.\right) = \frac{1}{2\pi\imath}\int_{\mathcal{C}} \frac{\prod_{j=1}^{m}\Gamma(b_j+z)\prod_{j=1}^{n}\Gamma(1-a_j-z)x^{-z}}{\prod_{j=n+1}^{p}\Gamma(a_j+z)\prod_{j=m+1}^{q}\Gamma(1-b_j-z)}\mathrm{d}z,$$

where the contour $\mathcal{C}$ is chosen in such a way that the poles of $\Gamma(b_j+z)$, $j=1,\ldots,m$, are separated from the poles of $\Gamma(1-a_j-z)$, $j=1,\ldots,n$.

By setting $m=K$ in (3.7), a lower bound $\mathcal{L}_{\mathrm{LB}}$ of $\mathcal{L}$ is obtained as

$$\mathcal{L}_{\mathrm{LB}} = \sum_{i=1}^{K}\varphi(\|\xi_i\|^2) \leq \mathcal{L}. \tag{3.11}$$

Integrating $\mathcal{L}_{\mathrm{LB}}$ over the joint density (3.8) with substitution $\|\xi_i\|^2 = y_i/K^n$, the lower bound of ergodic LSS is obtained. As indicated in [53], this integration can be greatly simplified by making use of a property of matrix permanent for order statistics. Namely, it was proven in [55] that if a joint density of ordered random variables $0 \leq y_K \leq \cdots \leq y_1 < \infty$ is written in the form $\mathrm{per}(h_j(y_i))$, $i,j=1,\ldots,K$, the corresponding unordered random variables, denoted by x_j, $j=1,\ldots,K$, are independent of each other with densities $h_j(x)$, $j=1,\ldots,K$. Clearly, for the joint density (3.8) the resulting density functions of the unordered and independent random variables are

$$h_j(x) = \frac{x^{j-1}}{\Gamma(j)^n}g_n\left(\sqrt{x}\right), \qquad j=1,\ldots,K. \tag{3.12}$$

Instead of dealing with random variables with non-trivial correlation as specified by a matrix permanent, we are dealing with independent random variables. As such, the lower bound of ergodic LSS can be calculated as

$$\mathbb{E}\left[\mathcal{L}_{\mathrm{LB}}\right] = \frac{1}{K}\sum_{j=1}^{K}\mathbb{E}\left[\varphi\left(\frac{x_j}{K^n}\right)\right] = \sum_{j=1}^{K}\int_0^\infty \frac{\varphi\left(x/K^n\right)x^{j-1}}{K\,\Gamma(j)^n}g_n\left(\sqrt{x}\right)\mathrm{d}x. \tag{3.13}$$

3.2.2 CLT of linear spectral statistics

Asymptotic spectral analysis using random matrix theory deals with LSS of large dimensional random matrices. The asymptotic result shows the

limiting behavior of $\mathcal{L}$ and is formally valid for matrices with infinite dimensions. However, a useful feature of the asymptotic result is that the statistics $\mathcal{L}$ converges to its limiting value $\mu_{\mathcal{L}}$ and the rate of convergence is fast as matrix dimensions increase. Therefore, the limiting LSS $\mu_{\mathcal{L}}$ serves as a good approximation for the expected value $\mathbb{E}[\mathcal{L}]$. By scaling with the dimension K_n, the fluctuation of a wide range of scaled LSSs, including the mutual information, is non-vanishing and converges to a limit. This result is useful when computing the asymptotic variance of the functional

$$X_{\mathcal{L}} = K_n(\mathcal{L} - \mu_{\mathcal{L}}) = K_n \int \varphi(\lambda) \mathrm{d}\left(\widetilde{F_{\mathbf{Q}}}(\lambda) - F_{\mathbf{Q}}(\lambda)\right), \tag{3.14}$$

where $F_{\mathbf{Q}}(\lambda)$ denotes the limiting eigenvalue distribution of $\mathbf{Q}$ as $K_i \to \infty$. Furthermore, the limiting distribution of $X_{\mathcal{L}}$ can be shown to be a Gaussian distribution for $\varphi(\lambda)$ that is analytic on the support of $F_{\mathbf{Q}}(\lambda)$, c.f. Proposition 2. This is the so-called Central Limit Theorem (CLT) for LSS of random matrix. The first work in this direction was done by Jonsson [56] for Wishart matrix and polynomial LSS. Further work was done by Johansson [57], Sinai and Soshnikov [58], Diaconis and Evans [59], Bai and Silverstein [60], Mingo and Nica [61], Breuer and Duits [62], among others. An direct application of the CLT for matrix ensembles is to approximate the distribution of the corresponding LSS with a Gaussian distribution. This only requires the expectation and variance of the LSS, which, in most of the cases, are much easier to obtain than the full distribution.

In the following, we assume $n = 2$ and use the limit $\lim_{K\to\infty}$ to denote the asymptotic regime

$$K_i \to \infty, \quad \text{with} \quad \theta = \frac{K_1}{K_2} \quad \text{and} \quad \zeta = \frac{K_0}{K_1} \quad \text{fixed.} \tag{3.15}$$

In the asymptotic regime (3.15), Silverstein [63] has shown that the ESD $\widetilde{F_{\mathbf{Q}}}(\lambda)$ converges almost surely to a non-random limiting distribution $F_{\mathbf{Q}}(\lambda)$. Such a convergence can be alternatively established via the convergence of resolvent $\widetilde{\mathcal{G}_{\mathbf{Q}}}(z)$ to the Cauchy transform $\mathcal{G}_{\mathbf{Q}}(z)$, defined as

$$\begin{aligned} \widetilde{\mathcal{G}_{\mathbf{Q}}}(z) &= \mathrm{tr}\left(\mathbf{I}_{K_2} z - \mathbf{Q}\right)^{-1} = \int \frac{1}{z-\lambda} \mathrm{d}\widetilde{F_{\mathbf{Q}}}(\lambda), \\ \mathcal{G}_{\mathbf{Q}}(z) &= \int_{\mathcal{S}_{\mathbf{Q}}} \frac{1}{z-\lambda} \mathrm{d}F_{\mathbf{Q}}(\lambda). \end{aligned} \tag{3.16}$$

Here, $z \in \mathbb{C}^+ = \{z : \mathrm{Im}(z) > 0\}$ and $\mathcal{S}_{\mathbf{Q}}$ denotes the support of $F_{\mathbf{Q}}(\lambda)$. Using multiplicative free convolution, Müller has shown in [11] that for any two unitary invariant random matrices whose entries are i.i.d. with

zero mean and unit variance, such as $\mathbf{H}_1$ and $\mathbf{H}_2$, the Cauchy transform of $\mathbf{Q} = \frac{1}{N_2}\mathbf{H}_2\mathbf{H}_1\mathbf{H}_1^\dagger\mathbf{H}_2^\dagger$ satisfies the cubic equation

$$z^2\mathcal{G}_{\mathbf{Q}}^3(z) + (\theta\zeta + \theta - 2)z\mathcal{G}_{\mathbf{Q}}^2(z) + \big((\theta\zeta - 1)(\theta - 1) - \theta z\big)\mathcal{G}_{\mathbf{Q}}(z) + \theta = 0. \quad (3.17)$$

Let us consider the fluctuations of the linear functional $X_{\mathcal{L}}$, defined as

$$\sigma_{\mathcal{L}}^2 = \mathbb{E}[X_{\mathcal{L}}^2] = K_2^2\,\mathbb{E}\left[(\mathcal{L} - \mu_{\mathcal{L}})^2\right]. \quad (3.18)$$

Applying an integral identity[2] [60, Eq. (1.14)] to (3.14), we obtain an alternative form of $X_{\mathcal{L}}$ given in terms of Cauchy transform $\mathcal{G}_{\mathbf{Q}}(z)$ and the resolvent $\widetilde{\mathcal{G}_{\mathbf{Q}}}(z)$

$$X_{\mathcal{L}} = \frac{1}{2\pi\imath}\oint_{\mathcal{C}} \varphi(z)G_K(z)\mathrm{d}z, \quad (3.19)$$

where $G_K(z) = K_2\left(\widetilde{\mathcal{G}_{\mathbf{Q}}}(z) - \mathcal{G}_{\mathbf{Q}}(z)\right)$. The complex integral on the right hand side of (3.19) is taken over any positively oriented closed contour $\mathcal{C}$ enclosing the support of $F_{\mathbf{Q}}(\lambda)$. After substituting (3.19) into (3.18), we obtain

$$\sigma_{\mathcal{L}}^2 = -\frac{1}{4\pi^2}\oiint_{\mathcal{C}_x,\mathcal{C}_y} \varphi(x)\varphi(y)\mathrm{Cov}\left(G_K(x), G_K(y)\right)\mathrm{d}x\mathrm{d}y, \quad (3.20)$$

where the contours $\mathcal{C}_x$ and $\mathcal{C}_y$ are non-overlapping and are taken in the same way as in (3.19). The operator $\mathrm{Cov}\left(G_K(x), G_K(y)\right) = \mathbb{E}\left[G_K(x)G_K(y)\right]$ refers to the covariance function of matrix resolvent scaled by the dimension K_2. The following result for the covariance function is derived in Publication VI using free probability theory for the second order limiting distribution of large random matrices.

Proposition 1. *The covariance function* $\mathrm{Cov}\left(G_K(x), G_K(y)\right)$ *is given by*

$$\mathcal{G}_{\mathbf{Q}}'(x)\mathcal{G}_{\mathbf{Q}}'(y)\mathcal{R}(\mathcal{G}_{\mathbf{Q}}(x), \mathcal{G}_{\mathbf{Q}}(y)) + \frac{\partial^2}{\partial x\partial y}\log\frac{\mathcal{G}_{\mathbf{Q}}(x) - \mathcal{G}_{\mathbf{Q}}(y)}{x - y}, \quad (3.21)$$

where $\mathcal{R}(x, y)$ *denotes the second order* R*-transform*

$$\mathcal{R}(x, y) = \frac{\mathcal{G}_{\mathbf{P}}'(1/x)\mathcal{G}_{\mathbf{P}}'(1/y)}{x^2y^2(\mathcal{G}_{\mathbf{P}}(1/x) - \mathcal{G}_{\mathbf{P}}(1/y))^2} - \frac{1}{(x - y)^2}, \quad (3.22)$$

and $\mathcal{G}_{\mathbf{P}}(z)$ *is the Cauchy transform of a Marčenko-Pastur distribution with parameter* ζ *as in (3.15)*

$$\mathcal{G}_{\mathbf{P}}(z) = \frac{1}{2} + \frac{1 - \zeta}{2z} - \sqrt{\frac{1}{4} - \frac{1 + \zeta}{2z} + \frac{(1 - \zeta)^2}{4z^2}}. \quad (3.23)$$

[2]The definition of Stieltjes transform in [60] is different from the Cauchy transform by a minus sign.

In literature, the covariance function $\mathcal{G}_{\mathbf{B}}(x,y)$ for the Wishart type $N\times N$ random matrix $\mathbf{B}=(1/N)\mathbf{X}^{\dagger}\mathbf{T}\mathbf{X}$ has been studied in [60], where $\mathbf{T}$ is a non-random Hermitian matrix and $\mathbf{X}$ is a Gaussian like[3] random matrix with i.i.d. entries. Therein, the correlation function of $\mathbf{B}$ has the form

$$\mathcal{G}_{\mathbf{B}}(x,y)=\frac{\mathcal{G}'_{\mathbf{B}}(x)\mathcal{G}'_{\mathbf{B}}(y)}{\left(\mathcal{G}_{\mathbf{B}}(x)-\mathcal{G}_{\mathbf{B}}(y)\right)^2}-\frac{1}{(x-y)^2}, \tag{3.24}$$

and it is subsequently used to derive an asymptotic variance of Rayleigh MIMO capacity in [64–66]. Note that the second term of (3.21) is exactly the same as (3.24) if $\mathbf{B}$ is replaced by $\mathbf{Q}=(1/K_2)\mathbf{H}_2\mathbf{P}\mathbf{H}_2^{\dagger}$ and it is assumed that $\mathbf{P}=\mathbf{H}_1\mathbf{H}_1^{\dagger}/K_1$ is non-random. Therefore, the variance $\sigma_{\mathcal{L}}^2$ of Rayleigh product ensemble has a different functional structure than for the Rayleigh MIMO matrix. The increased fluctuation of $X_{\mathcal{L}}$ is due to a non-zero second order R-transform $\mathcal{R}(x,y)$. For general discussion on the free probability theory, we refer to [67, 68]. The concept of second order limiting distribution and the relevant free probability machinery are established in [69–72] for various free random variables. The combinatorial explanations can be found in [61] via non-crossing permutations.

Based on the CLT for the Wishart type matrices [60, Lemma 1.1], we have proven in Publication VI the following CLT for the Rayleigh product ensembles with analytic function $\varphi(\cdot)$.

Proposition 2. *In the asymptotic regime (3.15), the linear functional $X_{\mathcal{L}}$ in (3.14) converges to a zero-mean Gaussian random variable with variance $\sigma_{\mathcal{L}}^2$ given by (3.20) and*

$$\mu_{\mathcal{L}}=\frac{1}{2\pi\imath}\oint_{\mathcal{C}}\varphi(z)\mathcal{G}_{\mathbf{Q}}(z)\mathrm{d}z. \tag{3.25}$$

Note that the CLT of LSS for the biorthogonal ensembles, such as the Rayleigh product ensemble, was proved by Breuer and Duits [62] for polynomial functions $\varphi(x)$. However, it is not clear how to extend this result for generic analytic functions $\varphi(x)$ such as the MI $\varphi(x)=\log(1+\bar{\gamma}x)$. Recently, the CLT for the product of two real and square random matrices was proven by Götze, Naumov, and Tikhomirov [73] for smooth function $\varphi(x)$.

[3]Each entry of the Gaussian like matrix has the same second and fourth moments as a Gaussian random variable.

3.3 Performance of cascaded MIMO channels

Using results for the LSS of Rayleigh product ensembles in Section 3.2, the information theoretical metrics of the presumed MIMO channel can be obtained. Here we consider two types of fading channels:

- Ergodic channel: The fading channel is random and takes independently a new value for each coherence time. The codeword spans over infinitely many coherence time periods.
- Non-ergodic channel: The fading channel is random and quasi-static. It remains constant over the transmission duration of the codeword as the length of codeword grows to infinity.

3.3.1 Ergodic mutual information and rate scaling law

When assuming ergodic channel, the transmitted codeword experiences all realizations of the fading channel $\mathbf{H}$. A reliable rate of communication $\mathbb{E}[\mathcal{I}]$, a.k.a. ergodic MI, can be achieved by coding over many independent fades of the channel.

It can be easily verified that the MI $\varphi(x) = \log(1+\bar{\gamma}x)$ fulfills the conditions of the inequality (3.7). Thus, a lower bound for the MI (3.4) is obtained as

$$\mathcal{I}_{\mathrm{LB}} = \sum_{i=1}^{K} \log(1+\bar{\gamma}\|\xi_i\|^2) \leq \mathcal{I} \tag{3.26}$$

where the channel dimensions $K_j = K$, $j = 0, \ldots, n$, are identical. By using the integral of Meijer's G-function [74, Eq. (21)] and the identity [75, Eq. (8.4.6.5)]

$$\log(1+x) = G_{2,2}^{1,2}\left(x \left| \begin{matrix} 1,1 \\ 1,0 \end{matrix} \right. \right), \tag{3.27}$$

the lower bound of ergodic MI can be calculated from (3.13) as

$$\mathbb{E}[\mathcal{I}_{\mathrm{LB}}] = \sum_{j=1}^{K} \frac{1}{\Gamma(j)^n} G_{n+2,1}^{2,n+2}\left(\frac{K^n}{\bar{\gamma}} \left| \begin{matrix} 0,1 \\ 0,0,i,\ldots,i \end{matrix} \right. \right). \tag{3.28}$$

An important property of the lower bound (3.28) is its asymptotic tightness when SNR goes to infinity. That is, as $\bar{\gamma} \to \infty$ the lower bound (3.26) becomes exact

$$\mathcal{I}_{\mathrm{LB}} = \log\left(\bar{\gamma}^K \prod_{i=1}^{K} \|\xi_i\|^2 \right) = \log\left(\bar{\gamma}^K \prod_{i=1}^{K} \lambda_i \right) = \mathcal{I}, \tag{3.29}$$

where we have used the fact that $\prod_{i=1}^{K}\|\xi_i\|^2 = \prod_{i=1}^{K}\lambda_i$.

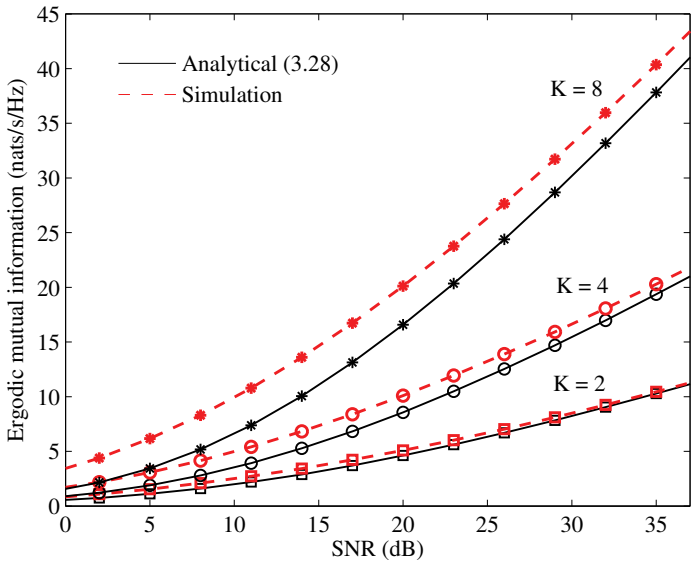

Figure 3.2. Ergodic MI of multiple cluster scattering MIMO channels assuming 3 clusters ($n = 4$). In all cases, the number of antennas equals the number of scatterers per cluster.

The scaling law for the ergodic MI in the high SNR regime can be understood using the result (3.13) and the asymptotic tightness property. Specifically, in the large SNR regime as $\bar{\gamma} \to \infty$, a simpler expression for the ergodic MI is obtained by replacing $\varphi(x) = \log(\bar{\gamma}x)$ in (3.13). Namely, we have

$$\mathbb{E}[\mathcal{I}] = nK\left(\sum_{i=1}^{K}\frac{1}{i} - \gamma_0 - 1\right) + K\log\left(\frac{\bar{\gamma}}{K^n}\right), \tag{3.30}$$

where $\gamma_0 = \lim_{K\to\infty}\left(\sum_{i=1}^{K} 1/i - \log K\right) \approx 0.5772$ is the Euler's constant. The per antenna rate scaling law at high SNR is obtained as

$$\lim_{K\to\infty}\frac{\mathbb{E}[\mathcal{I}]}{K} = \log(\bar{\gamma}) - n. \tag{3.31}$$

The scaling law (3.31) indicates that the per antenna ergodic MI scales as $\log(\bar{\gamma})$, and is a decreasing function of the number of clusters.

In Fig. 3.2, a 3-cluster ($n = 4$) scattering MIMO channel is considered with the number of scatterers per cluster being $K = 2,\ 4,$ and 8. The ergodic MI in nats/sec/Hz is plotted as a function of the received SNR. It is seen that the ergodic MI increases as the number of scatterers K (number of transceiver antennas) increases. This behavior is in line with the conventional MIMO channel model ($n = 1$), where increased spatial diversity (richness of the scattering) improves the ergodic MI [49].

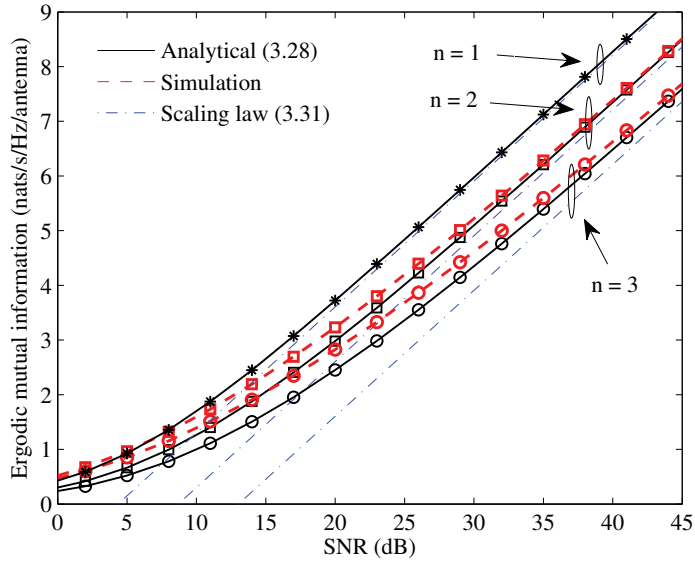

Figure 3.3. Per antenna ergodic MI of multiple cluster scattering MIMO channels assuming $K = 8$ with different numbers of clusters. In all cases, the number of antennas equals the number of scatterers per cluster. For $n = 1$ the analytical curve is obtained from the exact ergodic MI formula derived in [49]. For $n = 2, 3$ the analytical curves are obtained from the ergodic MI lower bound (3.28).

In Fig. 3.3, a scenario involving a fixed number of scatterers per cluster ($K = 8$) is considered with the number of clusters being 1 and 2. In addition, the conventional MIMO channel model ($n = 1$) has been considered. In order to verify the derived scaling law (3.31), we have plotted the per antenna ergodic MI as a function of the received SNR. It is observed that for a fixed SNR the ergodic MI decreases as the number of clusters increases. This observation is in agreement with the analytical scaling law (3.31). We also observe that the derived scaling law captures the behavior of the ergodic MI well at high SNR. As expected, we see from both figures that the lower bound (3.28) approaches the true value as the SNR increases.

3.3.2 Outage probability

Assuming a non-ergodic channel, the channel $\mathbf{H}$, albeit random, remains fixed for the duration of the transmitted codeword as the length of codeword grows to infinity. Without CSI at the transmitter, there is a non-zero probability, independent of the code length, that the MI (3.3) falls below any positive rate. The error probability corresponding to this rate cannot

be decreased exponentially with the code length [76]. In this case, no reliable transmission is possible and the performance cannot be evaluated using the ergodic MI. Instead, the fundamental limit for such a system can be explained using the rate versus outage tradeoff, characterized by the CDF of MI $\mathcal{I}$. Given a fixed rate r, the outage probability is defined as

$$P_{\text{out}}(r) = \Pr\{\mathcal{I} \leq r\} = F_{\mathcal{I}}(r), \tag{3.32}$$

where $F_{\mathcal{I}}(\cdot)$ denotes the CDF of $\mathcal{I}$.

By Proposition 2, the MI $\mathcal{I}$ of Rayleigh product channels with $n = 2$ is Gaussian in the asymptotic regime (3.15). Then the CDF $F_{\mathcal{I}}(r)$ can be approximated by the Gaussian distribution as

$$F_{\mathcal{I}}(r) \approx \frac{1}{2}\left(1 + \operatorname{erf}\left(\frac{r - K_2\mu_{\mathcal{I}}}{\sigma_{\mathcal{I}}\sqrt{2}}\right)\right) \tag{3.33}$$

and thus the outage MI is

$$\mathcal{I}_{\text{out}} \approx K_2\mu_{\mathcal{I}} + \sigma_{\mathcal{I}}\sqrt{2}\,\operatorname{erf}^{-1}(2P_{\text{out}} - 1), \quad P_{\text{out}} \in (0, 1). \tag{3.34}$$

In (3.33) and (3.34), $\mu_{\mathcal{I}}$ refers to the limiting MI (3.25) with $\varphi(x) = \log(1 + \bar{\gamma}x)$ for which a closed form expression can be found in [23, Coroll. 2]. In general case, it is difficult to obtain an explicit expression for the asymptotic variance $\sigma^2_{\mathcal{I}}$. However, when the transmitter and receiver have equal number of antennas, the expression of $\sigma^2_{\mathcal{I}}$ can be obtained by solving (3.20). The result is reported in Publication VI as

$$\sigma^2_{\mathcal{I}} = \log\frac{\bar{\gamma}(\omega_r - 1)^2}{\bar{\gamma} - \omega_r^2(2\omega_r - 2)}, \tag{3.35}$$

where $\omega_r \leq 0$ is the solution of the cubic equation

$$t^3 - 2t^2 + (1 - \bar{\gamma} + \bar{\gamma}\zeta)t + \bar{\gamma} = 0. \tag{3.36}$$

It is noted that the Gaussian convergence of MI $\mathcal{I}$ was established for possibly correlated and power-imbalanced multi-keyhole MIMO channels [21, 22], when two of the matrix dimensions (among K_0, K_1, and K_2) approach to infinity while the other one being fixed. However, there is a fundamental difference between the two MIMO models. Namely, the asymptotic capacity of MIMO channel in [21, 22] converges to the ergodic capacity with vanishing variance, while asymptotic variance (3.35) is non-vanishing in the asymptotic regime (3.15). Furthermore, as ratios of the matrix dimensions are not considered in [21,22], some key properties of the MIMO channels, such as the ergodic MI, cannot be differentiated for different finite matrix dimensions.

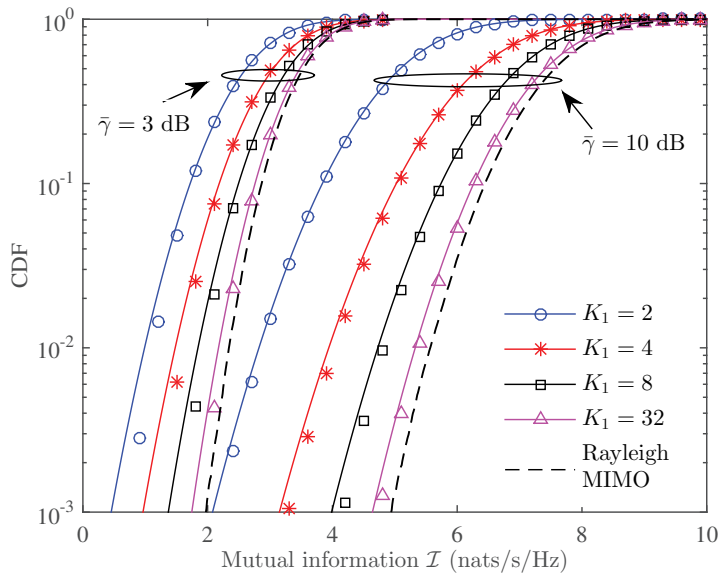

Figure 3.4. CDF of MI in the presence of 4×4 Rayleigh product channel. Solid line: Gaussian approximation (3.33); markers: simulations; dashed line: the CDF of MI in the presence of 4×4 Rayleigh MIMO channel.

In Fig. 3.4 the impact of the number of scatterers K_1 and the received SNR is studied, when a 4×4 MIMO system is considered in the presence of $K_1 = 2, 4, 8,$ and 32 scattering objects. We have plotted the approximative and empirical outage probability, the latter being obtained by numerical simulations. The outage probabilities are evaluated at SNRs $\bar{\gamma} = 3$ dB and $\bar{\gamma} = 10$ dB. For a comparison, we have also plotted the outage probability of a 4×4 Rayleigh MIMO channel with independent fading entries. As the number of scatterers (K_1) increases, the MI at a given probability level rapidly increases until K_1 is equal to the number of antennas. This phenomenon is especially visible when SNR is 10 dB. We recall that when the rank of the channel matrix is limited by the number of scatterers, increasing the number of scatterers effectively improves the rank of the channel matrix. When $K_1 > 4$, the matrix rank is limited by the number of antennas and the improvement of MI is relatively slow. Yet, the outage probability curve approaches to a limit, which corresponds to the outage probability of the independent Rayleigh MIMO channel as predicted in [22].

In Fig. 3.5 we have examined the impact of the number of antennas on the outage MI. We have plotted the approximative 1% outage MI (3.34) as a function of received SNR. We assume that the number of transmit

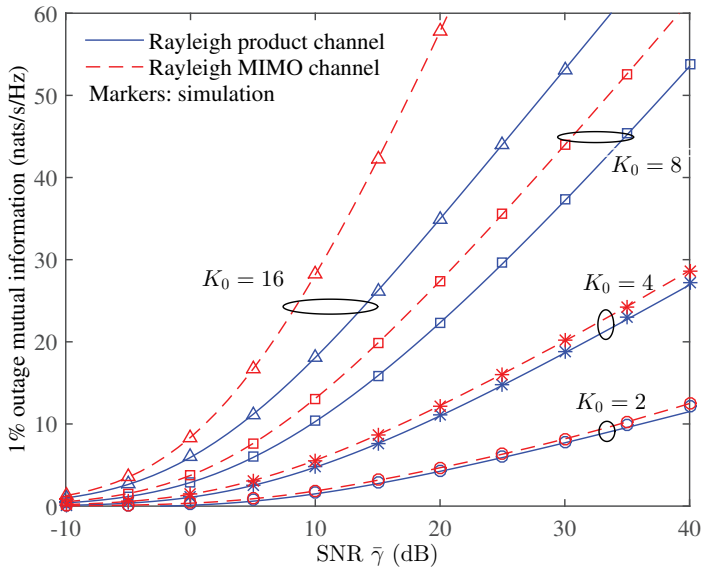

Figure 3.5. The 1% outage MI of Rayleigh product channels with $K_1 = 8$ scattering objects and equal numbers of antennas. Solid line: Gaussian quantile approximation (3.34); markers: simulations; dashed line: the outage MI of conventional Rayleigh MIMO channels with equal number of antennas.

and receive antennas are $K_0 = K_2 = 2, 4, 8,$ and 16 while the number of scatterers is fixed to 8. As expected, the outage MI for the Rayleigh product channel is lower than for the conventional Rayleigh MIMO channel due to the presence of a finite number of scatterers. In the high SNR regime, the outage MI curves of both channels attain the same slope when $K_0 \leq K_1$, which suggests that the MI scales at the same rate as the limiting Rayleigh MIMO channel. On the other hand, when $K_1 < K_0$ there is an increasing gap between the two channels as SNR increases. Finally, it is observed from Fig. 3.4 and 3.5 that the Gaussian approximation (3.33) and (3.34) is reasonably accurate for a wide range of parameter settings.

3.3.3 Finite-SNR diversity-multiplexing tradeoff

The concept of Diversity-Multiplexing Tradeoff (DMT) was originally proposed in [77] to characterize the diversity gain, related to the link reliability, and the multiplexing gain, related to the spectral efficiency. The DMT studied in [77] for asymptotic SNR indicates that both types of performance gains can be obtained simultaneously while satisfying a fundamental tradeoff. The DMTs for asymptotic SNR were later calculated for the Rayleigh product channel assuming a perfect receiver [20] as well as

a linear receiver [78]. The operational interpretation of the DMT framework is via the existence of universal codes, which are tradeoff optimal in the high SNR regime [79]. In space-time code design [80], DMT represents a useful analytical tool to characterize the asymptotic performance of codes. However, the asymptotic tradeoff provides a too optimistic upper bound to estimate the operational performance at realistic SNRs. Furthermore, recent works have shown that codes optimized for high SNR may not be optimal at low or moderate SNR [81]. Motivated by these facts, Narasimhan [81] proposed a finite-SNR DMT framework, which characterizes the non-asymptotic DMT at realistic SNR levels. In presence of correlated multi-keyhole MIMO channels, authors in [82] derived an approximation for the finite-SNR DMT, which is accurate when $K_0, K_2 \gg K_1$ at relatively high SNR levels. Assuming $K_1 = 1$, the exact tradeoff curve can be obtained by [51, Th. 2], where the DMT is calculated in the context of amplify-and-forward relay channels with single relay antenna. In Publication VI and VII, we obtained the finite-SNR DMT for Rayleigh product channels for a wide range of matrix dimensions at arbitrary SNR. It is noted that the considered DMT analysis may not be sufficient to characterize the performance of MIMO communications, since two different MIMO systems may have the same DMT, see e.g. [51, 82]. In this case, authors in [82] introduced the SNR offset and used it together with finite-SNR DMT to estimate the channel outage probability. Nevertheless, we restrict our discussion within the scope of DMT analysis as also been considered in [20, 48, 77, 78, 81] and one may resort to the asymptotic analysis in Section 3.3.2 to calculate the outage probability.

The multiplexing gain G_m of a MIMO channel is defined in [82, Eq. (21)] as

$$G_m = \frac{k}{\mu_{\mathcal{I}}} r, \tag{3.37}$$

where $k = \min(K_i)$, $i = 0, \ldots, n$. The multiplexing gain provides an indicator for the sensitivity of the rate adaptation strategy as the SNR changes. When the applied code attains a higher multiplexing gain, the rate adaptation tends to respond more dramatically on the SNR variations. At a fixed multiplexing gain, the finite-SNR diversity gain $G_d(G_m, \gamma)$ is defined as the negative slope of the log-log curve of outage probability $P_{\text{out}}(r)$ versus SNR with rate $r = G_m \, \mu_{\mathcal{I}}/k$,

$$G_d(G_m, \bar{\gamma}) = -\frac{\partial \log P_{\text{out}}(r)}{\partial \log \bar{\gamma}}. \tag{3.38}$$

At a particular SNR and multiplexing gain G_m, the diversity gain $G_d(G_m, \bar{\gamma})$

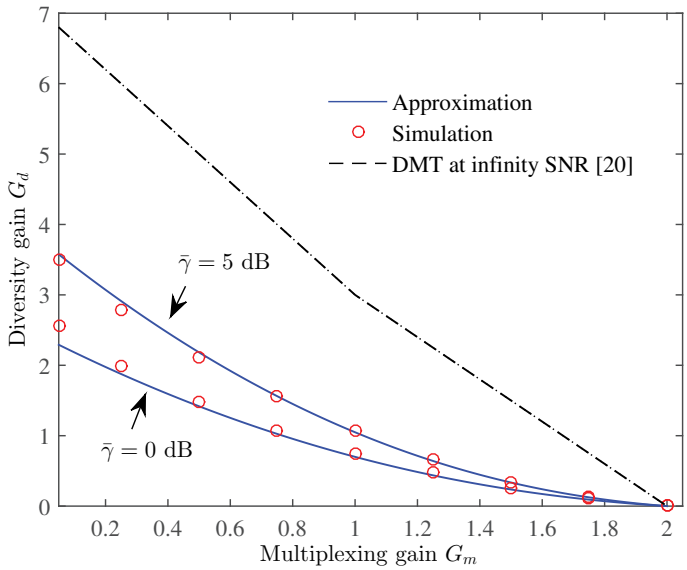

Figure 3.6. Finite-SNR DMT of a 4×4 Rayleigh product channel with $K_1 = 2$. Solid line: approximation; markers: simulations; dashed line: asymptotic DMT with SNR $\bar{\gamma} \to \infty$.

provides an estimate for the additional SNR needed to reduce the error probability by a certain amount. Using the approximated outage probability (3.33), the finite-SNR DMT can be obtained for the Rayleigh product channel when $n = 2$.

In Fig. 3.6 we have plotted the finite-SNR diversity gain as a function of multiplexing gain in the range $[0, 2]$ achievable for a 4×4 Rayleigh product channel with $n = 2$ and $K_1 = 2$. We have compared the approximated tradeoff curves with numerical simulations at SNRs $\bar{\gamma} = 0$ dB and $\bar{\gamma} = 5$ dB. Numerical results show that the proposed approximation accurately estimates the MIMO diversity at operational SNR levels. As the multiplexing gain approaches zero, the approximation error increases. This is due to the fact that the diversity gain at small G_m is characterized by the tail behavior of the outage probability, which is not captured by the Gaussian approximation (3.33) at finite matrix dimensions. For comparison purposes, we have also plotted the DMT of Rayleigh product channels according to [20, Eq. (8)], when SNR approaches infinity. It is clear that the asymptotic SNR DMT significantly overestimate the channel diversity at the considered SNR levels.

4. Conclusions

Radio signal propagation over wireless channels is subject to various electromagnetic mechanisms. In practical communication scenarios, these effects result in complicated multipath and shadowing phenomena. The statistical modeling provides an universal characterization for a wide range of wireless communication channels. It facilitates the performance analysis of communication systems operating over the wireless channels and enables optimal transceiver designs under certain statistical criterion. The so-called cascaded fading model serves as an extension to the basic statistical models and is shown to accurately capture some radio-wave propagation phenomena, such as lognormal shadowing, indoor signal propagations, and rank deficiency in multiantenna communications.

In this thesis, we described the linear transfer function of the cascaded fading channels with additive white Gaussian noise. In cases of single transceiver antenna and single scatterer, we studied the amplitude of the equivalent end-to-end channel as well as its physical motivation. With the channel state information available at the receiver only, the statistics of the cascaded channel amplitudes is equivalent to the multiplication of a sequence of random variables, each corresponding to the component channel. In Publication I, the distribution of products of Nakagami-m RVs was derived by utilizing a moment-based approximation. Using this result, we obtained in Publication II the outage probability of the cascaded Nakagami-m fading channels assuming non-trivial correlations among component channels. Furthermore, we considered in Publication III a cascaded Rician channel in the framework of the time-reversal transmission. The complex envelop of the received signal after time-reversal transmission was modeled as a product of two non-central complex Gaussian random variables. The distribution of the complex envelop, obtained via a bivariate Edgeworth expansion, was used to construct a blind time-

reversal detector in the presence of deterministic point target embedded in correlated multipath scattering. By capturing the multipath correlation, the proposed detector outperforms the blind time-reversal detector reported in literature.

When transceivers are equipped with multiple antennas and there are multiple scatterers in each cluster, the performance of the communication systems depends on the statistics of the eigenvalues of the end-to-end MIMO channels. For the cascaded Rayleigh MIMO channels, we focused on the MIMO mutual information assuming receiver side channel state information only. Using random matrix theory and free probability theory, we obtained the ergodic mutual information and outage probability under various MIMO settings. In Publication IV, a lower bound for the ergodic mutual information was obtained for cascaded square Rayleigh MIMO channels. The result indicates that the per antenna rate scales as $\log(\mathrm{SNR}) - n$, decreasing with the number of component channels n. In Publications V and VI, the asymptotic variance of mutual information was obtained for $n = 2$ in the large dimensional regime. Compared to the conventional Rayleigh MIMO channel with $n = 1$, the cascaded channels induce a higher asymptotic variance of mutual information due to increased eigenvalue fluctuation. In Publications VI and VII, the outage probability of the cascaded Rayleigh MIMO channel was proven to be Gaussian when channel dimensions grow to infinity. Using this result, a simple expression for the fundamental tradeoff between channel diversity gain and multiplexing gain was obtained. Results show that the known tradeoff curves for infinite SNR significantly overestimate the channel diversity gain when applied at realistic SNR levels.

References

[1] "Evolved Universal Terrestrial Radio Access (E-UTRA); LTE physical layer; General description (Release 10)," Tech. Rep. 3GPP Technical Specification 36.201 v10.0.0, Dec. 2010.

[2] "IEEE 802.16m System Description Document (SDD)," IEEE 802.16 Broadband Wireless Access Working Group, Tech. Rep. IEEE 802.16m-09/0034r2, Jan. 2009.

[3] D. Tse and P. Viswanath, *Fundamentals of Wireless Communication*. Cambridge: Cambridge University Press, 2005.

[4] M. K. Simon and M.-S. Alouini, *Digital Communication over Fading Channels*. New York: Wiley, 2000.

[5] V. Erceg, S. J. Fortune, J. Ling, A. J. Rustako, and R. A. Valenzuela, "Comparisons of a computer-based propagation prediction tool with experimental data collected in urban microcellular environments," *IEEE J. Sel. Areas Commun.*, vol. 15, no. 4, pp. 677–684, May 1997.

[6] J. B. Andersen, "Statistical distributions in mobile communications using multiple scattering," in *Proc. 27th URSI Gen. Assem.*, Maastricht, 2002.

[7] A. J. Coulson, A. G. Williamson, and R. G. Vaughan, "A statistical basis for lognormal shadowing effects in multipath fading channels," *IEEE Trans. Commun.*, vol. 46, no. 4, pp. 494–502, Apr. 1998.

[8] J. B. Andersen and I. Z. Kovacs, *Power distributions revisited*, Guildford, 2002.

[9] S. Saunders and A. Aragón-Zavala, *Antennas and Propagation for Wireless Communication Systems*, 2nd ed. Chichester: John Wiley & Sons, 2007.

[10] D. Gesbert, H. Bolcskei, D. A. Gore, and A. J. Paulraj, "Outdoor MIMO wireless channels: models and performance prediction," *IEEE Trans. Commun.*, vol. 50, no. 12, pp. 1926–1934, Dec. 2002.

[11] R. Müller, "A random matrix model of communication via antenna arrays," *IEEE Trans. Inf. Theory*, vol. 48, no. 9, pp. 2495–2506, Sep. 2002.

[12] D. Chizhik, G. J. Foschini, M. J. Gans, and R. A. Valenzuela, "Keyholes, correlations, and capacities of multielement transmit and receive antennas," *IEEE Trans. Wireless Commun.*, vol. 1, no. 2, pp. 361–368, Apr. 2002.

[13] R. Müller, "On the asymptotic eigenvalue distribution of concatenated vector-valued fading channels," *IEEE Trans. Inf. Theory*, vol. 48, no. 7, pp. 2086–2091, Jul. 2002.

[14] J. Salo, H. M. El-Sallabi, and P. Vainikainen, "The distribution of the product of independent Rayleigh random variables," *IEEE Trans. Antennas Propag.*, vol. 54, no. 2, pp. 639–643, Feb. 2006.

[15] G. K. Karagiannidis, N. C. Sagias, and P. T. Mathiopoulos, "N*Nakagami: a novel stochastic model for cascaded fading channels," *IEEE Trans. Commun.*, vol. 55, no. 8, pp. 1453–1458, Aug. 2007.

[16] N. C. Sagias and G. S. Tombras, "On the cascaded Weibull fading channel model," *J. Franklin Inst.*, vol. 344, no. 1, pp. 1–11, 2007.

[17] S. Ahmed, L.-L. Yang, and L. Hanzo, "Probability distributions of products of Rayleigh and Nakagami-m variables using Mellin transform," in *Proc. IEEE Int. Conf. Commun.*, Kyoto, Jun. 2011, pp. 1–5.

[18] Y. Chen, G. K. Karagiannidis, H. Lu, and N. Cao, "Novel approximations to the statistics of products of independent random variables and their applications in wireless communications," *IEEE Trans. Veh. Technol.*, vol. 61, no. 2, pp. 443–454, Feb. 2012.

[19] C. Zhong and T. Ratnarajah, "Ergodic sum rate analysis of Rayleigh product MIMO channels with linear MMSE receiver," in *Proc. IEEE Int. Symp. Inf. Theory*, St. Petersburg, Jul. 2011, pp. 2607–2611.

[20] S. Yang and J.-C. Belfiore, "Diversity-multiplexing tradeoff of double scattering MIMO channels," *IEEE Trans. Inf. Theory*, vol. 57, no. 4, pp. 2027–2034, Apr. 2011.

[21] G. Levin and S. Loyka, "On the outage capacity distribution of correlated keyhole MIMO channels," *IEEE Trans. Inf. Theory*, vol. 54, no. 7, pp. 3232–3245, Jul. 2008.

[22] ——, "From multi-keyholes to measure of correlation and power imbalance in MIMO channels: outage capacity analysis," *IEEE Trans. Inf. Theory*, vol. 57, no. 6, pp. 3515–3529, Jun. 2011.

[23] J. Hoydis, R. Couillet, and M. Debbah, "Asymptotic analysis of double-scattering channels," in *Proc. ASILOMAR'11*, Pacific Grove, CA, Nov. 2011, pp. 1935–1939.

[24] A. Firag, P. J. Smith, and M. R. McKay, "Capacity analysis of MIMO three product channels," in *Proc. Aust. Commun. Theory Work.*, Canberra, ACT, Feb. 2010, pp. 13–18.

[25] R. Müller and H. Hofstetter, "Confirmation of random matrix model for the antenna array channel by indoor measurements," in *Proc. IEEE Antennas Propag. Soc. Int. Symp.*, vol. 1, Boston, MA, USA, Jul. 2001, pp. 472–475.

[26] P. Almers, F. Tufvesson, and A. F. Molisch, "Keyhole effect in MIMO wireless channels: measurements and theory," *IEEE Trans. Wireless Commun.*, vol. 5, no. 12, pp. 3596–3604, Dec. 2006.

[27] H. Solomon and M. A. Stephens, "Approximations to density functions using pearson curves," *J. Am. Stat. Assoc.*, vol. 73, no. 361, pp. 153–160, Mar. 1978.

[28] H. Cramér, *Mathematical Methods of Statistics*. Princeton, NJ: Princeton University Press, 1999.

[29] D. Schleher, "Generalized Gram-Charlier series with application to the sum of log-normal variates," *IEEE Trans. Inf. Theory*, vol. 23, no. 2, pp. 275–280, Mar. 1977.

[30] R. Freedman, "On Gram-Charlier approximations," *IEEE Trans. Commun.*, vol. 29, no. 2, pp. 122–125, Feb. 1981.

[31] M. Abramowitz and I. A. Stegun, *Handbook of Mathematical Functions*. New York: Dover, 1972.

[32] M. B. De Kock, "Gaussian and non-Gaussian-based Gram-Charlier and Edgeworth expansions for correlations of identical particles in HBT interferometry," Ph.D. dissertation, University of Stellenbosch, 2009.

[33] S. B. Provost and H. Tae Ha, "On the inversion of certain moment matrices," *Linear Algebra Appl.*, vol. 430, no. 10, pp. 2650–2658, May 2009.

[34] G. Szegö, *Orthogonal Polynomials*, 4th ed. Providence: American Mathematical Society, 1939.

[35] R. N. Bhattacharya and R. R. Rao, *Normal Approximation and Asymptotic Expansions*. New York: Wiley, 1986.

[36] N. Balakrishnan, N. L. Johnson, and S. Kotz, "A note on relationships between moments, central moments and cumulants from multivariate distributions," *Stat. Probab. Lett.*, vol. 39, no. 1, pp. 49–54, Jul. 1998.

[37] I. Skovgaard, "On multivariate Edgeworth expansions," *Int. Stat. Rev.*, vol. 54, no. 2, pp. 169–186, Aug. 1986.

[38] B. Holmquist, "The d-variate vector hermite polynomial of order k," *Linear Algebra Appl.*, vol. 237-238, pp. 155–190, Apr. 1996.

[39] N. C. Beaulieu and K. T. Hemachandra, "Novel simple representations for Gaussian class multivariate distributions with generalized correlation," *IEEE Trans. Inf. Theory*, vol. 57, no. 12, pp. 8072–8083, Dec. 2011.

[40] I. S. Gradshteyn and I. M. Ryzhik, *Table of Integrals, Series, and Products*, 7th ed. New York: Academic Press, 2007.

[41] M. Fink, "Time reversal of ultrasonic fields. I. Basic principles," *IEEE Trans. Ultrason. Ferroelectr. Freq. Control*, vol. 39, no. 5, pp. 555–566, Sep. 1992.

[42] J. M. F. Moura and Y. Jin, "Detection by time reversal: single antenna," *IEEE Trans. Signal Process.*, vol. 55, no. 1, pp. 187–201, Jan. 2007.

[43] Y. Jin and J. M. F. Moura, "Time-reversal detection using antenna arrays," *IEEE Trans. Signal Process.*, vol. 57, no. 4, pp. 1396–1414, Apr. 2009.

[44] Y. Jin, J. M. F. Moura, and N. O'Donoughue, "Time reversal in multiple-input multiple-output radar," *IEEE J. Sel. Top. Signal Process.*, vol. 4, no. 1, pp. 210–225, Feb. 2010.

[45] N. O'Donoughue and J. M. F. Moura, "On the product of independent complex Gaussians," *IEEE Trans. Signal Process.*, vol. 60, no. 3, pp. 1050–1063, Mar. 2012.

[46] S. M. Kay, *Fundamentals of Statistical Signal Processing, Vol. II: Detection Theory*. Upper Saddle River, NJ: Prentice Hall, 1998.

[47] S. Jin, M. R. McKay, K. K. Wong, and X. Gao, "Transmit beamforming in Rayleigh product MIMO channels: capacity and performance analysis," *IEEE Trans. Signal Process.*, vol. 56, no. 10, pp. 5204–5221, Oct. 2008.

[48] S. Yang and J. C. Belfiore, "On the diversity of Rayleigh product channels," in *Proc. IEEE Int. Symp. Inf. Theory*, Nice, 2007, pp. 1276–1280.

[49] E. Telatar, "Capacity of multi-antenna Gaussian channels," *Eur. Trans. Telecommun.*, vol. 10, no. 6, pp. 585–595, Nov. 1999.

[50] N. Fawaz, K. Zarifi, M. Debbah, and D. Gesbert, "Asymptotic capacity and optimal precoding in MIMO multi-hop relay networks," *IEEE Trans. Inf. Theory*, vol. 57, no. 4, pp. 2050–2069, Apr. 2011.

[51] S. Loyka and G. Levin, "On outage probability and diversity-multiplexing tradeoff in MIMO relay channels," *IEEE Trans. Commun.*, vol. 59, no. 6, pp. 1731–1741, 2011.

[52] Z. Bai and J. W. Silverstein, *Spectral Analysis of Large Dimensional Random Matrices*. New York: Springer, 2006.

[53] G. Akemann and E. Strahov, "Hole probabilities and overcrowding estimates for products of complex Gaussian matrices," *J. Stat. Phys.*, vol. 151, no. 6, pp. 987–1003, Jun. 2013.

[54] H. Weyl, "Inequalities between the two kinds of eigenvalues of a linear transformation," *Proc. Natl. Acad. Sci. U. S. A.*, vol. 35, no. 7, pp. 408–411, Jul. 1949.

[55] R. Vaughan and W. Venables, "Permanent expressions for order statistic densities," *J. R. Stat. Soc. Ser. B*, vol. 34, no. 2, pp. 308–310, 1972.

[56] D. Jonsson, "Some limit theorems for the eigenvalues of a sample covariance matrix," *J. Multivar. Anal.*, vol. 12, no. 1, pp. 1–38, Mar. 1982.

[57] K. Johansson, "On fluctuations of eigenvalues of random Hermitian matrices," *Duke Math. J.*, vol. 91, no. 1, pp. 151–204, Jan. 1998.

[58] Y. Sinai and A. Soshnikov, "Central limit theorem for traces of large random symmetric matrices with independent matrix elements," *Bull. Math. Soc.*, vol. 29, no. 1, pp. 1–24, Mar. 1998.

[59] P. Diaconis and S. Evans, "Linear functionals of eigenvalues of random matrices," *Trans. Am. Math. Soc.*, vol. 353, no. 7, pp. 2615–2633, 2001.

[60] Z. D. Bai and J. W. Silverstein, "CLT for linear spectral statistics of large-dimensional sample covariance matrices," *Ann. Probab.*, vol. 32, no. 1A, pp. 553–605, Jan. 2004.

[61] J. A. Mingo and A. Nica, "Annular noncrossing permutations and partitions, and second-order asymptotics for random matrices," *Int. Math. Res. Not.*, vol. 2004, no. 28, pp. 1413–1460, Jan. 2004.

[62] J. Breuer and M. Duits, "Central limit theorems for biorthogonal ensembles and asymptotics of recurrence coefficients." [Online]. Available: http://arxiv.org/abs/1309.6224

[63] J. Silverstein, "Strong convergence of the empirical distribution of eigenvalues of large dimensional random matrices," *J. Multivar. Anal.*, vol. 55, no. 2, pp. 331–339, Nov. 1995.

[64] M. A. Kamath and B. L. Hughes, "The asymptotic capacity of multiple-antenna Rayleigh-fading channels," *IEEE Trans. Inf. Theory*, vol. 51, no. 12, pp. 4325–4333, Dec. 2005.

[65] A. M. Tulino and S. Verdú, "Asymptotic outage capacity of multiantenna channels," in *Proc. ICASSP'05*, Philadelphia, PA, 2005, pp. 825–828.

[66] M. Debbah and R. Müller, "MIMO channel modeling and the principle of maximum entropy," *IEEE Trans. Inf. Theory*, vol. 51, no. 5, pp. 1667–1690, May 2005.

[67] D. Voiculescu, "Addition of certain non-commuting random variables," *J. Funct. Anal.*, vol. 66, no. 3, pp. 323–346, May 1986.

[68] R. Speicher, "Free probability and random matrices," in *Proc. Int. Congr. Math. Vol. III*, S. Y. Jang, Y. R. Kim, D.-W. Lee, and I. Yie, Eds., Seoul, Korea, 2014, pp. 477–501.

[69] J. A. Mingo and R. Speicher, "Second order freeness and fluctuations of random matrices: I. Gaussian and Wishart matrices and cyclic Fock spaces," *J. Funct. Anal.*, vol. 235, no. 1, pp. 226–270, Jun. 2006.

[70] J. A. Mingo, P. Śniady, and R. Speicher, "Second order freeness and fluctuations of random matrices: II. Unitary random matrices," *Adv. Math. (N. Y).*, vol. 209, no. 1, pp. 212–240, Feb. 2007.

[71] B. Collins, J. A. Mingo, P. Śniady, and R. Speicher, "Second order freeness and fluctuations of random matrices. III: Higher order freeness and free cumulants," *Doc. Math.*, vol. 12, pp. 1–70, 2007.

[72] O. Arizmendi and J. A. Mingo, "Second order even and R-diagonal operators, in preparation."

[73] F. Götze, A. Naumov, and A. Tikhomirov, "Distribution of linear statistics of singular values of the product of random matrices." [Online]. Available: http://arxiv.org/abs/1412.3314

[74] V. S. Adamchik and O. I. Marichev, "The algorithm for calculating integrals of hypergeometric type functions and its realization in REDUCE system," in *Proc. ISSAC'90*, Tokyo, Japan, 1990, pp. 212–224.

[75] A. Prudnikov, Y. A. Brychkov, and O. I. Marichev, *Integrals and Series. Volume 3: More Special Functions*. Amsterdam: Gordon and Breach, 1990.

[76] L. Ozarow, S. Shamai, and A. Wyner, "Information theoretic considerations for cellular mobile radio," *IEEE Trans. Veh. Technol.*, vol. 43, no. 2, pp. 359–378, May 1994.

[77] L. Zheng and D. N. C. Tse, "Diversity and multiplexing: a fundamental tradeoff in multiple-antenna channels," *IEEE Trans. Inf. Theory*, vol. 49, no. 5, pp. 1073–1096, May 2003.

[78] C. Zhong, T. Ratnarajah, Z. Zhang, K.-K. Wong, and M. Sellathurai, "Performance of Rayleigh-product MIMO channels with linear receivers," *IEEE Trans. Wireless Commun.*, vol. 13, no. 4, pp. 2270–2281, Apr. 2014.

[79] S. Tavildar and P. Viswanath, "Approximately universal codes over slow-fading channels," *IEEE Trans. Inf. Theory*, vol. 52, no. 7, pp. 3233–3258, Jul. 2006.

[80] P. Elia, K. R. Kumar, S. A. Pawar, P. V. Kumar, and H. F. Lu, "Explicit space-time codes achieving the diversity-multiplexing gain tradeoff," *IEEE Trans. Inf. Theory*, vol. 52, no. 9, pp. 3869–3884, Sep. 2006.

[81] R. Narasimhan, "Finite-SNR diversity-multiplexing tradeoff for correlated Rayleigh and Rician MIMO channels," *IEEE Trans. Inf. Theory*, vol. 52, no. 9, pp. 3965–3979, Sep. 2006.

[82] S. Loyka and G. Levin, "Finite-SNR diversity-multiplexing tradeoff via asymptotic analysis of large MIMO systems," *IEEE Trans. Inf. Theory*, vol. 56, no. 10, pp. 4781–4792, Oct. 2010.

Errata

Publication I

In Fig. 1, the CCDF curves with triangular markers should refer to the case $\rho = 0.3$.

Publication IV

In the integrand of (10), the factor of the first product in the denominator should be $\Gamma(a_j + z)$, not $\Gamma(a_j + s)$.

Publication V

The Cauchy transform of $\mathbf{P}$ in (9) should be

$$G_{\mathbf{P}}(z) = \sqrt{\frac{1}{4} - \frac{1+\zeta}{2z} + \frac{(1-\zeta)^2}{4z^2}} - \frac{1}{2} - \frac{1-\zeta}{2z}.$$

Aalto-DD 209/2015

ISBN 978-952-60-6562-5 (printed)
ISBN 978-952-60-6563-2 (pdf)
ISSN-L 1799-4934
ISSN 1799-4934 (printed)
ISSN 1799-4942 (pdf)

Aalto University
School of Electrical Engineering
Department of Communications and Networking
www.aalto.fi

BUSINESS + ECONOMY

ART + DESIGN + ARCHITECTURE

SCIENCE + TECHNOLOGY

CROSSOVER

DOCTORAL DISSERTATIONS